ACCELERATED CORROSION LABORATORY STUDIES IN FERROCEMENT

A DISSERTATION

Submitted in partial fulfilment of the requirements for the award of the degree of

MASTER OF ENGINEERING

in

CIVIL ENGINEERING

With Specialization in

BUILDING SCIENCE & TECHNOLOGY

By

SEEMA KAUSHAL

DEPARTMENT OF CIVIL ENGINEERING
UNIVERSITY OF ROORKEE
ROORKEE-247667 (INDIA)

JANUARY, 1994

CANDIDATE 'S DECLARATION

I, hereby, certify that the work which is being presented in the dissertation **"ACCELRATED CORROSION LABORATORY STUDIES IN FERROCEMENT"** in partial fulfilment of the requirements for the award of degree of **MASTER OF ENGINEERING** with specialization in **BUILDING SCIENCE AND TECHNOLOGY**, submitted in the Department of Civil Engineering, University of Roorkee, is an authentic record of my own work carried out for a period from September '93 to January '94 under the supervision of **Dr.S.K.Kaushik**, Professor, **Dr.Anand Prakash**, Professor and **Er. V.K.Gupta**, Reader, Department of Civil Engineering, University of Roorkee, Roorkee.

The matter embodied in this dissertation has not been submitted for the award of any other degree or diploma.

Seema Kaushal

Date : 31st Jan., 1994 **SEEMA KAUSHAL**

This is to certify that the above statement made by the candidate is correct to the best of our knowledge.

Er. V.K.Gupta	**Dr. Anand Prakash**	**Dr. S.K.Kaushik**
Reader	Professor	Professor

Department of Civil Engineering
University of Roorkee
ROORKEE - 247667

Date : 31st Jan., 1994

ACKNOWLEDGEMENT

I wish to express my deep sense of gratitude to my honourable guides **Dr. S.K.Kaushik**, Professor, **Dr. Anand Prakash**, Professor, and **Er. V.K.Gupta**, Reader, Civil Engineering Department, University of Roorkee, Roorkee, for their invaluable guidance, utmost help and constant encouragement throughout the dissertation, which cannot be acknowledged in a few words. I am equally obliged to **Dr. V.K.Tewari**, Reader, Metallurgical Department, University of Roorkee, Roorkee and **Mr. Awadhesh Kumar** for their help.

I am grateful to **Mr. K.C.Khurana** and **Mr. M.S.Gupta** and other staff of the Test Hall Concrete laboratory and Structural Engineering Section of the Civil Engineering Department, University of Roorkee, Roorkee , for their immense help and co-operation.

I am very thankful to my friend **Ms.Preeti Malik (FROOTI)** for her constant help and moral support.

ABSTRACT

Ferrocement has gained wide popularity as an efficient form of construction material over the past two decades preferentially for thin-walled plane and spatial structures. Ferrocement constructions need special care and caution to ensure satisfactory performance over the expected service life, leaving little room for poor workmanship.

Because of the similarity in the nature of the ingredients of conventional concrete and ferrocement, the durability characteristics are expected to be similar even though the mechanical characteristics may be quite different. Limited data is available on factors affecting the durability of ferrocement and for predicting its service behaviour.

The aim of this study was to investigate the corrosion behaviour of 224 ferrocement elements, 400mm x 200mm x 20mm in size, by subjecting them to accelerated corrosion using 0%, 3%, 6% and 9% salt solutions (NaCl) for curing the samples under submerged and alternate wetting and drying conditions. The specimens were exposed to these environments for 1, 3, 7, 14, 21, 28 and 60 days. The effect of degree of corrosion on the flexural strength of ferrocement was then studied. Typical wire samples were studied under microscope to assess the nature and extent of corrosion.

The results obtained from the study indicate that corrosion shows a tendency of stabilizing after some time. The rate of corrosion or the corroding influences have little effect on the first cracking strength of the specimens. The cummulative corrosion, as measured by md value, does not result in any

appreciable loss in the cracking strength unless md assumes a very high value. Effort has been made to co-relate the non-destructive spontaneous potential test results i.e. the electrical half-cell potential of steel in cement mortar to the extent of corrosion.

The future of ferrocement and its extended uses will depend on finding satisfactory solution to the durability aspects.

LIST OF FIGURES

LIST OF TABLES

LIST OF PLATES

LIST OF SYMBOLS

σ_{crb} : First cracking stress in bending

S_{LT} : Specific surface of the reinforcement in the tension zone

σ_{mr} : Modulus of rupture of the mortar

σ_{ub} : Ultimate tensile stress in bending

SB : Submerged condition

AW : Alternate wetting and drying condition

C_e : Extent of (or cumulative) corrosion [measured in md]

C_r : Rate of corrosion [measured in mdd]

md : Loss in weight in milligrams per square decimeter surface area of the mesh wires .

mdd : md per day

mV_{sce} : Spontaneous potential in millivolts as measured using a standard calomel electrode.

mVcse : Spontaneous potential in millivolts as measured using a copper-copper sulphate electrode.

mVshe : Spontaneous potential in millivolts as measured using a standard hydrogen electrode.

d : Diameter of the mesh wire

W_o : Original weight of 10 cm length mesh wire

W_f : Final weight of 10 cm length sample mesh wire

CHAPTER - I

INTRODUCTION

1.1 GENERAL

The developments in ferrocement as a construction material and the related technology transfer over the past two decades has resulted in extensive research inputs and innovative applications. Ferrocement initially used for boat building during World War II is today being extensively used for housing, marine, rural, agricultural and sanitation applications, especially in the developing countries.

According to ACI committee 549, "Ferrocement is a type of thin walled reinforced concrete construction where usually a hydraulic cement is reinforced with layers of continuous and small diameter wire meshes. The meshes may be of metallic material or other suitable materials." Thus ferrocement is a kind of composite material where the filler material, usually brittle in nature, called matrix is reinforced with fibers dispersed throughout the composite resulting in better structural performance than that of individual one.

Ferrocement exhibits a behaviour so different from the conventional reinforced concrete in performance, strength and potential applications that it must be classed as a separate material. It is made of rich cement-sand mortar and reinforced primarily with several layers of wire mesh and skeletal steel, if required. The layers of mesh are placed parallel to each other across the thickness of element. The dispersion of the fibers in the brittle matrix causes improvement in many of the engineering properties of the material such as fracture, tensile and flexural strengths, toughness, fatigue and impact resistance and also provides advantages in terms of fabrication of products and

components and their economy. It also has the advantage of being mouldable and of one piece construction requiring no heavy plant and machinery.

1.2 HISTORICAL DEVELOPMENT

The history of ferrocement goes back to the year 1848 when Joseph Lambot of France constructed several rowing boats, plant pots, seats and other items from a material that he called "Ferricement".

During its early period of development the Dutch also built reinforced mortar barges of 50 to 60 tons capacity for carrying ashes and refuse on canals.

During 1940's Nervi , an Italian architect resurrected the original idea of Lambot and used it to construct small tonnage vessels, the largest being the 165 tons motor sailor "Irene". During World War II a number of ferrocement crafts were built by the Italian Navy.

The first application of ferrocement to Civil Engineering Structures was made by Nervi and Bartoli in 1947 in the construction of an experimental storage shed of size 10.7m x 21.3m, only 44.45mm thick. In 1948 , the Exposition Hall in Turin was the first public structure constructed with ferrocement.

In the Soviet Union, the first ferrocement structure built was a vaulted roof over a shopping centre on Reshetnikov street in Leningrad in 1958. Techniques such as vibro-bending and vibro-pressing have also been used for precast ferrocement products.

In Sri lanka, a ferrocement house resistant to cyclones was developed and constructed, capable of withstanding a wind speed of 140 mph.

In Brazil, ferrocement has been used by architect Lima at Salvador city for the urbanization of slums, schools, and factories. A code of practice on ferrocement has also been developed.

In Cuba, ferrocement technology has been used by the fishing fleet since 1960's. Several swimming pools have been constructed which are partially cast-in-situ and partially pre cast.

In Bangladesh, ferrocement technology was introduced in early 1970's mainly in the fields of building components such as flooring, roofing, and walling units, door-windows frames, beam-column formworks, watertanks and fishing boats.

The Indian space research organization (ISRO) have made use of ferrocement in the construction of partially underground cable trenches, elevated circular twin watertanks, perforated slabs for aeration towers, roof panels for passenger bus shelters - cantilever and folded plate type. Economy to the tune of 35% to 60% has been achieved.

Structural Engineering Research Centre (SERC), Ghaziabad, U.P., has been a premier research institution engaged in the development of ferrocement technology. This technology has been released to more than 50 firms for commercial exploitation in India through National Rural Development Corporation (NRDC), and 35 of these are already in production.

Many other countries like Thailand, Malaysia, Indonesia, Philippines, Australia, Nepal, etc. have been using the technology and experiences as distributed by the International Ferrocement Information Centre (IFIC), Bangkok, Thailand.

1.3 CONSTITUENTS OF FERROCEMENT

The thickness of ferrocement elements varies from 10 to 50mm. The minimum mesh reinforcement ratio is 0.3%, and generally the

total volume of steel lies between 1% to 8% of the structural element. The cover of the outermost layer of wires is usually 2 to 5mm.

The high compressive strength of the mortar is obtained using high cement content and low water-cement ratio. The usual mix proportions are 1:1.5 to 1:3 cement:sand. Water-cement ratio is mostly kept between 0.35 to 0.5 by weight. The desired compressive strength of mortar for ferrocement structures is in excess of 25 N/mm^2.

The general constituent materials of ferrocement are cement, sand, water, wire mesh, skeletal steel and suitable admixtures.

1.3.1 Cement

The cement used in ferrocement is normally ordinary portland cement, conforming to IS:269-1976 or ASTM standard C-150. The cement should be fresh and of uniform consistency . For construction in an electrochemically active environment like sea water, it may be necessary to use sulfate-resisting cement.

1.3.2 Fine Aggregate

The aggregate normally used is natural sand and the grading of the particles, if possible, should comply with IS:383-1970 grading zone II for fine aggregates or ASTM standard C-35, as given in Table 1.1 . The sand should be clean, hard, strong and free of organic impurities and with a fineness modulus between 2.2 to 2.8

TABLE 1.1 : SIEVE ANALYSIS OF FINE AGGREGATE

Sieve size	Percentage passing IS:383-70 (ZONE-II)	ASTM	SERC
4.75mm	90-100	95-100	100
2.36mm	75-100	80-100	99.25
1.18mm	55-90	50-85	89.75
600μ	35-59	25-60	58.00

300μ	8-30	10-30	14.00
150μ	0-10	2-10	1.25

1.3.3 Water

Generally potable water is fit to be used for mixing the mortar provided it is clean and free from such impurities that may interfere with the setting of cement and adversely affect the strength or cause corrosion of the reinforcement. According to the IS:456-1978 specifications, the permissible limits of impurities in mixing water are as follows :-

(i) To neutralize 200ml sample of water, using phenolphthalin as an indicator, it should not require more than 2ml of 0.1 normal NaOH.

(ii) To neutralize 200ml sample of water, using methyl orange as an indicator, it should not require more than 10ml of 0.1 normal HCl.

(iii) Permissible limits for solids are as given in Table 1.2 .

(iv) The pH value of water should not be less than 6.

(v) Sea water should not be used for mixing or curing.

TABLE-1.2 : PERMISSIBLE LIMITS FOR SOLIDS IN WATER

Impurity	Max Value (mg/l)
Organic	200
Inorganic	300
Sulfates	500
Chlorides	1000
Suspended matter	2000

1.3.4 Admixtures

(i) The conventional and high range water reducing

admixtures (superplasticizers) should conform to ASTM C:494-1971. Decrease in water content results in lower shrinkage and less surface crazing.

(ii) Mineral admixtures (e.g. flyash) conforming to ASTM C:618-1985 can be added to cement to increase workability and durability.

(iii) Air-entraining admixtures conforming to ASTM C:260-1986 can be used to increase resistance to freezing and thawing.

(iv) Addition of silica fume is reported to reduce porosity and improve strength, permeability and durability.

1.3.5 Wire Mesh

Wire mesh generally consists of thin wires of diameter ranging from 0.5 to 1.5 mm, woven, welded or twisted into a mesh with a spacings of 5 to 25 mm. The meshes to be used in ferrocement should be easy to handle and flexible enough to be bent at sharp corners. The mechanical behaviour of ferrocement is highly dependent upon the type, quantity, orientation and strength properties of the mesh. The mesh opening may be square, rectangular or hexagonal shaped or expanded metal mesh. The various types of meshes generally used are shown in Fig.-1.1

1.3.6 Skeletal Steel

Skeletal steel is normally used for making the framework of the structure upon which the layers of mesh are laid. Both the longitudinal and transverse rods of mild steel, high tensile steel or G.I. wires (3 to 5 mm dia.) are evenly distributed and shaped to form. If the spacing is more than 30cm, it is not treated as a structural reinforcement and often serves as spacer rods to the mesh reinforcement.

1.4 APPLICATIONS OF FERROCEMENT

Since it is possible to cast very thin sections with ferrocement, there is saving in basic materials, i.e. cement and steel, along with the requirement of only a low level of labour skill. Because of its reduceddead weight, the handling and erection of ferrocement elements is easier, thereby making it suitable for prefabrication. Prefabricated prestressed corrugated ferrocement elements present interesting architectural and structural potentialities. Above all ferrocement suits well to those structures that owe their strength to form such as thin shells and corrugated surfaces. Ferrocement is specially useful in developing countries like India. For details see Table 1.3 .

1.5 PROBLEM FORMULATION

Introduction

The reinforcing mesh in ferrocement is liable to corrosion like steel in a conventionally reinforced concrete structure. Even at working loads, these structures develop micro cracks in the outermost fibers. This deterioration of the cover material results in corrosion of the reinforcing metallic material. In turn, corrosion of reinforcement adds to the destruction of the cover by spalling or bursting due to an increase in the volume of the corrosion products formed inside the cover, thus aggravating the corrosion process.

Ferrocement elements are remarkably thin with small cover to the mesh. The mesh wires also have small diameters. In view of these, apprehensions regarding the durability and service life of ferrocement structures naturally arise. The aim of this study is to investigate the corrosion behaviour of ferrocement elements.

Investigations have been carried out on 224 ferrocement

strips, 400mm x 200mm x 20mm in size, showing varying degrees of corrosion after a lapse of 1,3,7,14,21,28 and 60 days of immersion (submerged and alternate wetting & drying conditions) in salt solutions of 0%, 3%, 6% and 9% concentrations. The effect of degree of corrosion on the flexural strength of ferrocement has been studied.

1.6 THESIS ORGANIZATION

The concept, historical development, constituent materials, applications and problem formulation are highlighted in Chapter-I.

Chapter-II deals with the literature review on investigations and theoretical developments on the subject.

Chapter-III describes the experimental programme for casting, different curing conditions and then testing of specimens for corrosion studies. The information about materials, specimen details and test set-ups is also given. The results of the tests conducted are presented in the last section of the chapter.

Chapter-IV deals with the discussion of the results obtained.

Chapter-V includes conclusion and scope for further work.

Table 1.3 : APPLICATIONS OF FERROCEMENT

Field	Application
(i) Buildings	Flooring, roofing & walling units; Door & window frames; Beam-column formworks; Waterproof linings for roofs, chajjas & swimming pools; Repair of corroded and damagedconcrete members; Domes, vaults and catenaries; Pipes and conduits.
(ii) Water Supply & Sanitation Services	Overhead and storage water tanks; Prefabricated modules; Ferrocement septic and sedimentation tanks; Pipes.
(iii)Agriculture	Irrigation channel units; Canal linings; Storage tanks for grains, seeds, fertilizers, edible oil, etc.;Fermentation tanks for cocoa coffee, wine, beer & fish sauses; Cattle feeders; Water troughs.
(iv) Energy	Biogas digesters and holders; Solar energy plant components; Natural gas cooling towers.
(v) Marine	Fishing and cargo boats; Pontoons and coracles; Buoys and docks; Submarine structures; Off-shore tanker terminals; Floating bridges; Floating shelters for flood prone areas.
(vi) Miscellaneous	Surfacing for soil-cement based rural roads; Cyclone resistant shelters; Chimneys and flues; Ovens and fire places; Power poles; Linings for tunnels; Water proofing treatment; Gas tanks; Bus shelters; Decorative panel tiles; etc. .

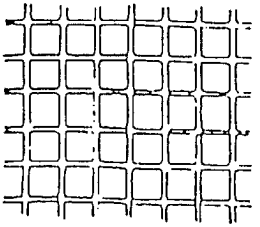

a. Welded Mesh

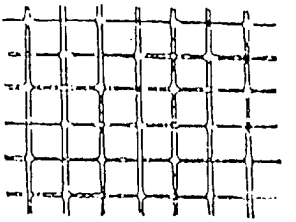

b. Woven Mesh

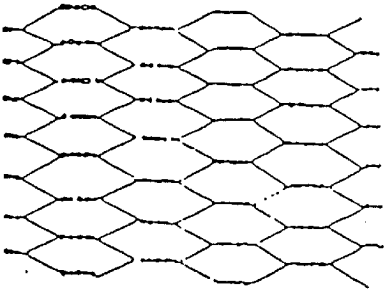

c. Chicken Mesh

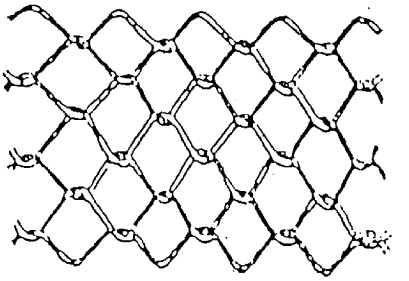

d. Chain Link

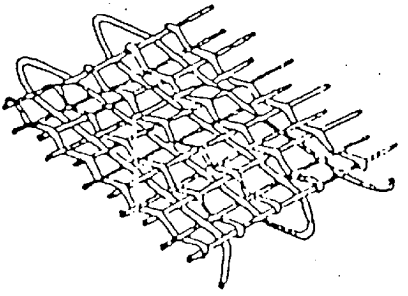

e. Watson MeSH

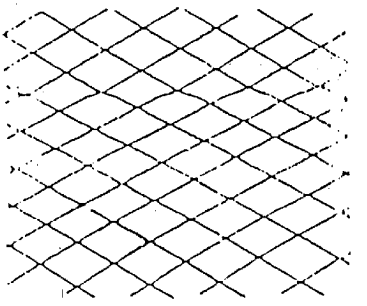

f. Expanded Metal

Fig 1.1 different types of meshes used in ferrocement

CHAPTER - II

LITERATURE REVIEW

2.1 GENERAL

Research investigations into the behaviour of ferrocement has revealed that its mechanical properties depend on the volume fraction and specific surface of mesh reinforcement, tensile strength of mortar, yield strength of wire mesh, modulus of elasticity of mortar and wire mesh, bond strength between mortar and mesh, reinforcement and the mortar cover. A brief review of its behaviour in flexure and durability & corrosion studies is presented in this chapter.

2.2 FERROCEMENT IN FLEXURE

The behaviour of ferrocement in flexure is governed by the combined influence of factors that affect its behaviour in tension and compression . Collen and Kirwan (1) and Rao and Gowder (2) investigated the behaviour of ferrocement in flexure by varying the amount of mesh reinforcement. Desayi and Jacob (3) observed that the ultimate flexural strength of ferrocement increases with an increase in mesh-mortar parameter.

Logan and Shah (4) carried out tests on ferrocement beams reinforced with varying sizes and layers of welded mesh and found that the first cracking stress in bending (σ_{crb}) in the extreme mortar fibre was linearly related to the specific surface of the reinforcement in the tension zone (S_{LT}) as given below :

$$\sigma_{crb} = 28.02\ S_{LT} + \sigma_{mr} \quad \text{in MPa} \qquad (2.1)$$

where S_{LT} is the specific surface in mm^{-1} ; and σ_{mr} is the modulus of rupture of the mortar in MPa.

Johnston and Mowat (5) carried out tests on ferrocement beams 150mm wide, 914mm long, 25mm thick and reinforced with meshes of

different types and orientations. The geometry and orientation of the reinforcement was found to have a marked effect on the strength of systems reinforced with expanded metal and welded mesh. For a given effective steel content, and by implication cost, the order of performance for uniaxial bending is expanded metal, standard bars, welded mesh and woven mesh.

Surya Kumar and Sharma (6) from their tests on ferrocement beams found that the ultimate and first crack strengths of the composite increase linearly with an increase in the percentage area of mesh reinforcement. Based on their test results, the following empirical equations were obtained for extreme fibre tensile stress of the composite at first crack and ultimate failure.

$$\sigma_{crb} = 1.96\ p_m + 3.33 \qquad \text{in MPa} \qquad (2.2)$$

$$\sigma_{ub} = 7.26\ p_m + 3.33 \qquad \text{in MPa} \qquad (2.3)$$

Balguru, Naaman and Shah (7) conducted test on ferrocement beams to predict deflection and crack width. The experimental load-deflection curves consisted of three distinct stages : (i) a steep linear portion before cracking of mortar ; (ii) after the first cracking of mortar but before yielding of mesh ; and (iii) after yielding of meshes when the slope becomes almost parallel to the deflection axis (Fig.2.1) .

Yen and Su (8) studied the influence of skeletal steel on the flexural behaviour of ferrocement. The effect of skeletal steel on the first crack moment was found to be negligible. However, the presence of skeletal steel increased the ultimate moment capacity and ductility of the composite.

Mansur and Paramasivam (9) investigated the behaviour of ferrocement beams by varying the volume fraction of reinforcement and

water-cement ratio of mortar and found that both the first crack and ultimate moments increased with an increase in either the matrix grade (by decreasing the water-cement ratio) or the volume fraction of reinforcement. For a given volume fraction of reinforcement, a lower grade matrix gave a larger number of cracks with smaller crack widths. However, as the load approached the ultimate value, the cracks opened up more rapidly. For a given grade of matrix, a higher volume fraction of reinforcement provided a more effective control of crack width.

Kaushik et. al (10) compared the behaviour of simply supported and horizontally restrained ferrocement beams. The restrained beams showed an increase in the first crack moment and ultimate moment capacity and decrease in ultimate deflection, crack spacing and crack widths as compared to the simply supported beams.

2.3 DURABILITY AND CORROSION OF FERROCEMENT

The successful performance of ferrocement in an aggressive environment depends to a great extent on its durability against the environment rather than on its strength properties. For ferrocement to be durable, its component materials, i.e. mortar and wire mesh should retain their bond and strength and shouldn't disintegrate over a period of time. The disintegration of mortar is due to volume changes caused by various weathering agents such as cyclic thermal changes and alternate wetting and drying. The action of aggressive chemicals on hardened cement paste, particularly sulfates, cause volume changes and cracking in the mortar. The mesh reinforcement is normally protected by the alkalinity of the rich and dense mortar and the cover. The cover in ferrocement is about 2mm to 5mm and this increases the corrosion risk to mesh reinforcement.

To prevent corrosion, galvanized wire mesh is commonly

used. The use of galvanized wire mesh along with ungalvanized skeletal steel bars creates the galvanic cell problem. Christensen and Williamson (11) were the first to identify this problem and also gave the solution. They suggested the use of Chromium trioxide at the rate of 100-300ppm by weight of water in preparing the mortar. If the cracks are not wider than 0.1mm, Greenius (12) found that corrosion was not severe even when the depth of cover was 0.5mm . From his extensive tests, limiting the water-cement ratio seemed to be adequate for satisfactory performance under sea water exposure. Naaman and Sabnis (13) suggested a net cover of 2mm .They even suggested a smaller depth of cover for those ferrocement elements in which reinforcement was galvanized, surface painting was used and low limiting crack width was adopted. Bigg (14) also suggested the use of galvanized wire mesh.

During the last decade, the corrosion and durability aspects of ferrocement have been extensively investigated by several researchers. Mathews, Achyutha and Rao (15) subjected cracked ferrocement specimens to accelerated corrosion tests by alternate wetting and drying in sea water for 30 days. They found that the ultimate tensile strength of the specimens with initial crack widths of about 0.05mm and 0.10mm was reduced by 4% and 12% respectively.

Trikha et. al (16) investigated the extent of corrosion in 12 ferrocement structures of various types with ages ranging from 6 to 12 years. They concluded that in mechanically cast ferrocement structures using galvanized steel wire mesh and well graded sand for mortar, corrosion was only mild with or without protective coating. However, inadequate cover, bad compaction and poor workmanship all lead to an increase in the incidence and rate of corrosion.

Selvi Rajkumari et. al (17) studied the corrosion

resistance of polymer impregnated ferrocement and unimpregnated ferrocement specimens. Accelerated corrosion tests were performed by subjecting the specimens to alternate drying and wetting in salt water (3.5% NaCl). The corrosion damage of unimpregnated ferrocement specimens was found to be nearly 10 times more than in the polymer impregnated ferrocement specimens.

Chowdhury and Nimityongskul (18) studied the corrosion in cracked and uncracked ferrocement specimens by subjecting them to alternate wetting and drying in sea water and urine. The depth of mortar was the main variable and a considerable improvement in corrosion protection was obtained by increasing the depth of cover from 1mm to 3mm. Very small improvement was obtained beyond 4mm. The intensity of corrosion was higher in case of urine as compared to sea water.

Ravindrarajah and Paramasivam (19) studied the effects of alternate wetting and drying in sea water and of curing in 6% NaCl solution on strength and stiffness of ferrocement in direct tension and flexure. The test results indicated that the ultimate strength and stiffness of ferrocement were not affected by 1000 cycles of wetting and drying in sea water or by exposing in 6% NaCl solution for 9 weeks. However, the first crack strength showed improvement due to maturity gain for the mortar component.The ferrocement specimens which were initially subjected to first crack load, did not suffer any loss in the ultimate strength due to the above exposure conditions.

Yozuqullu (20) studied the durability of sulphur impregnated ferrocement specimens. These specimens were found to be practically impermeable with a noticeable increase in strength together with an improved resistance against acid attack.

The durability of ferrocement can also be improved by

mixing an acrylic latex solution (21) in the mortar used for the final plastering. It was found that coating the ferrocement surfaces with appropriate paints (22) also improves its durability.

Tashiro and Ueoka (23) measured the spontaneous potential between cement paste and reinforced steel for detecting the existence of corrosion of steel in specimens having various mix proportions and cured for 150 days. They justified the validity of the method on the ground that corrosion of steel can be attributed to the destruction of the passive state of steel and the consequent electric potential changes. When the value of the spontaneous potential is smaller than -300mV or when it rapidly rises , corrosion occurs. ASTM C:876-91 standardizes the test method for measurement of half-cell potentials of uncoated reinforcing steel in concrete using Copper-Copper sulphate half cell instead of the Calomel electrode as used by Tashiro and Ueoka .

2.4 THE CORROSION PHENOMENON (16,24)

Corrosion of steel in a medium is a spontaneous process which is electrochemical in nature and can be explained by the following reactions :

- Anodic reaction

$$Fe \text{ ------> } Fe^{2+} + 2e \qquad \ldots(1)$$

Cathodic reactions

$$2H^{+} + 2e \text{ -----> } 2H \text{ -----> } H_2 \qquad \ldots(2)$$

(Hydrogen evolution in the absence of air)

$$O_2 + 2H_2O + 4e \text{ ------> } 4(OH)^{-} \qquad \ldots(3)$$

(Oxygen reduction in the presence of air)

In both cases, the liquid around the cathode becomes more highly alkaline. The reactions 2 and 3 take place mainly in acidic and alkaline medium respectively .

The rust formation takes place when oxygen comes into contact with iron ions dissolved at the anode according to reaction 1 and results in forming insoluble $Fe_2O_3.nH_2O$ (iron rust) according to the following reaction :

$$2Fe^{2+} + 1/2\ O_2 + 4(OH)^- + (n-2)H_2O \text{ ----> } Fe_2O_3.nH_2O \quad ..(4)$$

A pH value of more than 11.5 is needed for the protective film formation on the steel surface and fresh concrete to act as an anodic inhibitor, also impeding the cathode reaction which requires the presence of oxygen. The effects of alkalinity on iron passivation can be seen in the Pourbaix diagram (Fig.2.2) (24). For a 25 C temperature, the potential of iron corrosion may varies from (+0.1)V to (-0.4)V, depending on the permeability of mortar and on the chloride levels. Between these values, a pH higher than 9.0 leads to a passivation region in the Pourbaix diagram .

The cement mortar must prevent reinforcement from corrosion by constituting a physical and chemical barrier to inhibit the formation of electrochemical cells. Physical protection is provided by the mechanical resistance and impermeability of the mortar to aggressive agents. Chemical protection is a function of the alkalinity of mortar due to reactions of tricalcium and dicalcium silicates which produce a great amount of calcium hydroxide, $Ca(OH)_2$. The calcium hydroxide, with a pH of around 12.6, dissolves in water filling the voids and capillaries of the mortar making it alkaline. Thus, a good cement mortar provides a protective environment to steel reinforcement against corrosion.

The rate of corrosion of reinforcing steel may be reported either by the weight loss of metal in milligrams per square decimeter of surface area per day (mdd) or by metal penetration in cms

of penetration per year (cpy) excluding any adherent or non-adherent corrosion products on the surface.

2.4.1 Cover Carbonation

High alkalinity, mainly given by calcium hydroxide may be reduced through the years by the action of carbon dioxide (CO_2) in the atmosphere and by other acidic gases. This phenomenon is called carbonation which occurs according to the main reaction :

$$Ca(OH)_2 + CO_2 \text{ -----> } CaCO_3 + H_2O \qquad \ldots(5)$$

Calcium carbonate ($CaCO_3$) precipitates at a pH value of around 9.4, thus modifying the passivation action of cement mortar on steel.

A fully water-saturated mortar does not carbonate; the same applies for a completely dry one. There is an optimum level of humidity (50%-70%) which maximizes the speed of carbonation. Very high humidity makes it difficult for the acid gases to penetrate the mortar, a very low humidity does not allow the reaction to occur as there is a lack of water. The depth of the carbonation increases very quickly in the beginning, and then more slowly, when it tends asymptotically to a maximum value. Thus an alternate wetting and drying cycle would accelerate the process of corrosion.

2.4.2 Chloride Effect

Chloride is the most common, potentially aggressive agent incorporated in mortar as it constitutes the basis of admixtures which accelerate the hardening process. Chlorides may also occur in aggregates, in contaminated water and in cleaning products. The Cl^- ion reduces mortar resistivity and may also destroy the passive conditions which were created because of the alkaline environment. This causes the corrosion process to be accelerated.

$$Fe^{3+} + 3Cl^{-} \text{ -----> } FeCl_3 \quad \ldots(6)$$

and by hydrolysis,

$$FeCl_3 + 3(OH)^{-} \text{------> } 3Cl^{-} + Fe(OH)_3 \quad \ldots(7)$$

The chloride ion acts only as a reaction catalyst. It is not consumed and the process is permanent. A small amount of chloride can cause large corrosion. The Cl^{-} ion, when in an electrolyte, alters the Pourbaix equilibrium diagram as it causes the area of passivity region to become smaller. Chloride concentrations equal to or higher than 700mg/litre break the passive protection of the steel when in limewater with pH equal to 12.5 .Thus, any level of chloride is harmful to ferrocement. There is ,however, great disagreement among authors concerning the acceptable levels of chloride for reinforced concrete (for ferrocement, information on this area is lacking) . Some authors state that levels higher than 0.1% in relation to the cement weight would be harmful, while others contend that levels lower than 1.5% are not risky.

2.5 CONCLUDING REMARKS

The performance of ferrocement in terms of durability and the related loss of strength is not well known upto now. For an extensive use of ferrocement units as applicable to low income and rural requirements of our developing nation, there is a need to know the useful life of ferrocement structures in different environments with some certainity. Thus, a study has been carried out to simulate accelerated corrosion conditions in the laboratory to quantitatively assess the residual strength of a ferrocement unit.

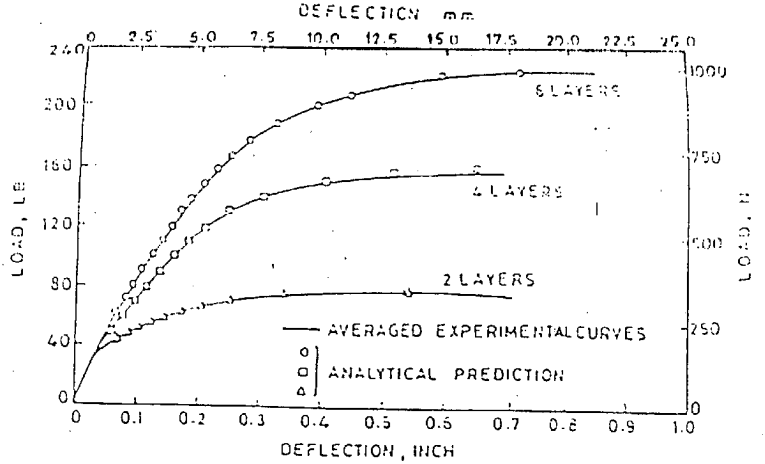

Fig 2·1 comparison of analytical and experimental load-deflection curves of specimens with ½" welded-mesh. * author [7]

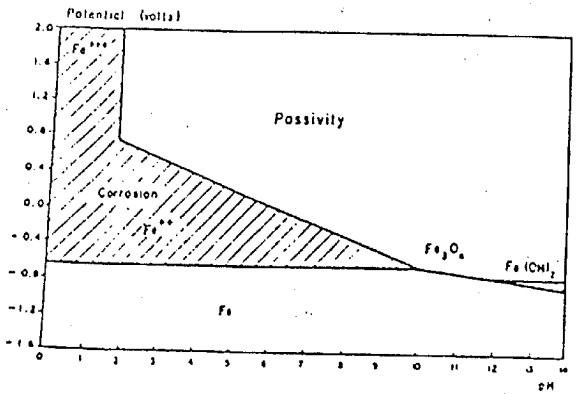

ig 2·2 pourbaix diagram: potential pH system for $Fe-H_2O$ at 25°C. * author [24]

CHAPTER - III

EXPERIMENTAL PROGRAMME

3.1 GENERAL

The aim of the present investigation was to conduct a systematic corrosion study on 20mm thick ferrocement strips. Due to a short period of study, in which corrosion of widely varying magnitudes was to be generated, the specimens were subjected to accelerated corrosion tests. The extent and rate of corrosion were studied along with the loss in the flexural strength of the composite.

In all, 224 ferrocement specimens were cast with the following specifications :-

SIZE	: 400mm x 200mm
THICKNESS	: 20mm
CEMENT MORTAR	: (a) 1:1.5
	(b) 1:3
WATER-CEMENT RATIO	: 0.5
MESH REINFORCEMENT	: 2 layers of 22 SWG Galvanized Square Woven Mesh with 7mm mesh size
COVER TO REINFORCEMENT	: 5mm
SKELETAL STEEL	: None

The sample dimensions and reinforcement details are shown in Fig.3.1. Two companion specimens were cast for each case to obtain an average value.

In order to achieve accelerated corrosion, Sodium chloride solutions of different concentrations have been used. The details of the different curing conditions are as follows :-

CURING SOLUTIONS : (a) Potable water - 0%

(b) NaCl solution - (i) 3%

(ii) 6%

(iii)9%

CURING CONDITIONS : (a) Submerged (SB)

(b) Alternate wetting & drying (AW)-24hr.cycle*

PERIOD OF CORROSION : (a) 1 day

(b) 3 days

(c) 7 "

(d) 14 "

(e) 21 "

(f) 28 "

(g) 60 "

* The 24 hour cycle has been followed for all the samples subjected to alternate wetting and drying except for the 1 day period samples in whose case 8 hours if wetting and 16 hours of drying has been followed.

The samples have been designated as shown below :-

(Sand - to Cement ratio)/(% of curing solution)/(Period of corrosion)/(Curing condition)

For e.g.: 1.5/0/60/SB designates a sample that has been cast using 1:1.5 cement-sand mortar and has been cured for 60 days in potable water (i.e. 0% solution) under submerged condition.

3.2 MATERIALS

The materials used for casting of ferrocement samples are cement, fine aggregates, wire mesh and water. The specifications of the materials as obtained from laboratory tests are given below.

3.2.1 Cement

The cement used in the experimental work was ordinary portland cement conforming to IS:269-76 . The result of the various tests conducted on the cement used are given in Table 3.1 .

TABLE 3.1 : PHYSICAL PROPERTIES OF CEMENT

S.No.	Test Conducted	Test Result	IS:269-76
1.	Colour	Moderate Grey	
2.	Normal Consistency (%)	29.5	30
3.	Initial Setting Time (minutes)	30	30 min.
4.	Final Setting Time (minutes)	70	600 max.
5.	Compressive Strength (MPa)		
	(i) 3 days	20.6	16
	(ii) 7 days	28.0	22

3.2.2 Fine Aggregate

The fine aggregate consisted of a mixture of fine river sand and coarse quartz sand in the ratio 2:1 by weight. The fineness modulus of mixed sand was 2.31 .The sieve analysis of the mixed sand is shown in Table 3.2 .

TABLE 3.2 : SIEVE ANALYSIS OF FINE AGGREGATE (EXPERIMENTAL)

S.No.	Sieve Size	Percentage passing	ACI 549 Committee req.
1.	4.75mm	100	100
2.	2.36mm	100	80-100
3.	1.18mm	81	50-85
4.	600μ	61	25-60
5.	300μ	18	10-30
6.	150μ	9	2-10

Fineness Modulus = 2.31

3.2.3 Water

Potable tap water was used in the casting and curing of the specimens and as well as the control mortar cubes .

3.2.4 Cement Mortar

Two kinds of mortar mixes were used in the fabrication of the samples -1:1.5 and 1:3; keeping the water-cement ratio fixed at 0.5. The properties of the hardened cement mortars used are given in Table 3.3 .

TABLE 3.3 : PROPERTIES OF HARDENED MORTARS

Mix	Compressive Strength 3 , 7 & 28 days (MPa)	Water Absorption (%)	Modulus of Elasticity (GPa)
1:1.5	15.05, 18.4, 28.05	3-4	11.921
1:3	12.0, 17.4, 26.12	3-6	11.093

3.2.5 Reinforcing Mesh

Two layers of 22 SWG Galvanized square woven wire mesh with a mesh opening of 7mm was used .The properties of the mesh used are:

WIRE DIAMETER	= 0.75mm
MESH OPENING	= 7 mm
YIELD STRESS	= 365 MPa
ULTIMATE TENSILE STRENGTH	= 399.3 MPa
ELONGATION	= 16 %
MODULUS OF ELASTICITY	= 148 GPa

3.2.6 Mould

The ferrocement plates were cast horizontally in

rectangular timber moulds of inner size 400mm x 200mm with a thickness of 20mm. A minimum cover of 5mm on all sides was maintained when placing the reinforcement inside the mould.

3.3 CASTING OF SPECIMENS

Wire mesh pieces of size 390mm x 190mm were cut from the 900mm wide rolls. These pieces were rolled in the opposite direction, spread flat on the floor and pressed to obtain flat pieces.

The specimens were cast horizontally on the cleaned flat floor of the test hall. First a plastic sheet was laid on the surface and the rectangular timber mould placed on it. The floor sheet and the sides of the mould were oiled for easy demoulding after casting.

The required quantities of materials were weighed and then dry mixed using trowels and spade. The weighed quantity of water was then added to the dry mix. The mortar was mixed vigorously till the resulting mix became homogeneous and uniform in appearance.

A mortar layer of 4-6 mm thickness was spread uniformly throughout in the mould. Then the first layer of the mesh was placed in position followed by a second mortar layer. The second layer of wire mesh was laid on the mortar and thereafter, the final layer of mortar was applied.

The mortar was compacted using a plate vibrator. The top surface of the sample was smoothened first with a timber float and then finished with a steel float.

3.4 CURING OF SPECIMENS

The samples were demoulded after 24 hours of casting and then placed in a water tank for another 24 hours. The samples were then placed in the tanks of respective NaCl concentrations i.e. 0%, 3%, 6%

and 9% . For the samples subjected to alternate wetting and drying, a cycle of 24 hours of wetting and 24 hours of drying under atmospheric conditions was followed, except for the samples that were exposed to only 1 day corrosion period. Such samples were wetted for 8 hours and then air dried for 16 hours.

3.5 TESTS AND PROCEDURES

All the specimens were subjected to the following sequence of tests (in the chronological order) :

(a) Flexural Strength test

(b) Standard Potential test

(c) Extent of Corrosion test (Weight loss and diameter reduction measurements)

(d) Visual Inspection under Microscope

3.5.1 Flexural Strength Test

The ferrocement strips have been tested in flexure under central loading as shown in Fig.3.2 and Plate 3.1. The test was conducted using a 40 ton capacity hydraulically operated Universal Testing Machine (UTM) in the Concrete test laboratory. The two sample supports for the specimen consisted of roller points welded to I-sections resting on the base of UTM. A roller (for the single point loading) was fixed at midspan of specimen using a paste of plaster of paris and allowed to set for about 15 minutes. Plywood packings between support rollers and the specimen and the plaster of paris for the loading roller have been used to overcome any unevenness in the surface finish of the sample for uniform distribution of load and bearing . The sample was then placed on the supports after giving plywood packings and load was applied on the roller. The first crack load of the composite was noted for all the specimens. The close up of a

sample in the ultimate state is shown in Plate 3.2 .

In order to measure the longitudinal strain on the bottom surface of some samples (midspan central extreme fibre on the tension side), 65 mm Bekalite electrical strain gauges (of resistance 118.1 $\pm$ 0.2 Ω) were pasted gently after cleaning the surface with sand paper and acetone. At each increment of loading, strain gauge readings were taken by an electrical strain gauge indicator with a least count of 1 micro strain. To measure the vertical deflection at midspan for some samples, a dial gauge (of least count 0.01mm) with a magnetic base was placed on the steel base.

3.5.2 Standard Potential Test

This test method covers the estimation of the electrical half-cell potential of uncoated reinforcing steel in the field and the laboratory, for the purpose of determining the corrosion activity of the reinforcing steel. When the value of the spontaneous potential is larger negatively than -300 mV or when it rapidly rises, corrosion occurs.

The spontaneous potential of specimens was measured by the use of a micro-voltmeter, a Calomel electrode and Platinum wire. The circuit diagram used is shown in Fig.3.3 .The mild steel wire mesh exposed due to the destructive flexural test was welded to a platinum wire and electrically connected to the positive terminal of the voltmeter. Prewetting of the specimen surface was done at the point of its contact with the calomel electrode by saturated KCl solution. The results obtained have been given later in the chapter.

3.5.3 Corrosion Study

To assess the degree or extent of corrosion, 6 samples of wires of 100 mm length were taken out of each sample. The samples were drawn from both the meshes at the centre and the sides after extracting

the meshes from the hardened mortar. To find the loss in the weight of a sample wire as compared to the original value, the wire was cleared off the corrosion products first mechanically followed by dissolving it in an acidic solution with an inhibitor. The weight measurements were recorded using an Electronic Weighing Balance. The readings of the reduced diameter of the sample wires were also taken using a screw gauge.

3.5.4 Visual Inspection

Some of the wires were also studied under a microscope in the Metallography Laboratory in the Metallurgical Department. Photographs of the typical samples taken under the microscope (magnified about 25 and 40 times) are given in Plates 3.3-3.16 .

3.6 PRESENTATION OF RESULTS

(i) First Crack Load

The experimental values of the first crack load and the calculated cracking stress are given in columns 3 and 4 of Tables-3.4 & 3.5 . The first crack strength of the composite has been determined as the extreme fibre stress in the strip due to flexure to cause initial cracking by the ordinary beam flexural formula. A sample calculation is given in Appendix-I.

(iv) Midspan Deflections

The vertical deflections at midspan for specimens 1.5/9/28/AW-2, 3/0/7/SB-1 and 3/0/14/AW-2 are given in columns 3,4 and 5 respectively of Table-3.6 .

(v) Tensile Strain

The tensile extreme fibre strain at midspan for the specimens 1.5/9/28/AW, 3/0/7/SB, 3/0/14/AW, 3/3/14/SB and 1.5/0/21/SB are given in columns 3, 4, 5, 6 and 7 of Table-3.7 .

(vi) Spontaneous (Half-Cell) Potential

The half cell potential values (in calomel scale) are given in columns 3, 4, 5 and 6 of Tables-3.8 & 3.9 . The conversion of the potential values to different scales is given in the Appendix-II.

(vii)Weight Loss

The net weight after corrosion and the weight loss values (of 100mm extracted and cleaned wire samples) for all the specimens are given in columns 4 and 5 respectively of Tables-3.10 & 3.11 .

(viii)Reduced Diameters

The diameter values of the sample wires are given in column 3 of Tables-3.10 & 3.11 . The calculated values of cumulative corrosion C_e and the rate of corrosion C_r are given in columns 7 and 8 of Tables-3.10 & 3.11 .

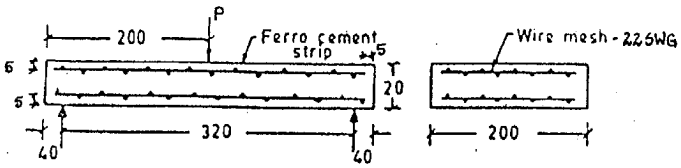

(All dimensions in mm)

Fig 3·1 sample dimensions and reinforcement details

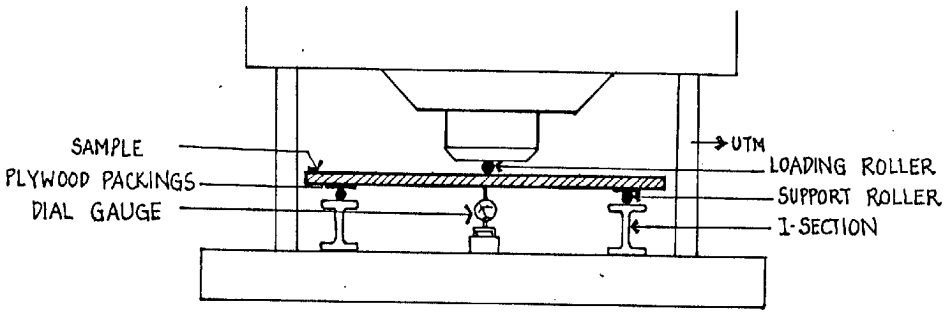

Fig 3·2 flexural strength test set-up

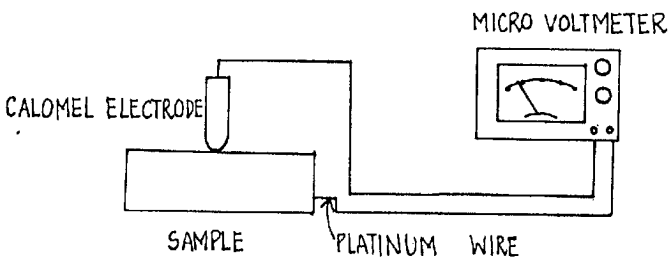

Fig 3·3 standard potential test set-up

TABLE 3.4 : FLEXURAL STRENGTH TEST RESULTS - 1:1.5 MIX

S. No.	Sample	First Crack Load (kg)	First Cracking Strength (MPa)
1.	1.5/0/1/SB	90	5.27
2.	1.5/0/1/AW	100	5.86
3.	1.5/3/1/SB	80	4.69
4.	1.5/3/1/AW	100	5.86
5.	1.5/6/1/SB	110	6.44
6.	1.5/6/1/AW	110	6.44
7.	1.5/9/1/SB	80	4.69
8.	1.5/9/1/AW	100	5.86
9.	1.5/0/3/SB	120	7.03
10.	1.5/0/3/AW	140	8.20
11.	1.5/3/3/SB	100	5.86
12.	1.5/3/3/AW	110	6.44
13.	1.5/6/3/SB	130	7.62
14.	1.5/6/3/AW	120	7.03
15.	1.5/9/3/SB	120	7.03
16.	1.5/9/3/AW	120	7.03
17.	1.5/0/7/SB	170	9.96
18.	1.5/0/7/AW	150	8.79
19.	1.5/3/7/SB	160	9.37
20.	1.5/3/7/AW	150	8.79

Contd.....

Continued

21.	1.5/6/7/SB	160	9.37
22.	1.5/6/7/AW	160	9.37
23.	1.5/9/7/SB	150	8.79
24.	1.5/9/7/AW	160	9.37
25.	1.5/0/14/SB	180	10.55
26.	1.5/0/14/AW	180	10.55
27.	1.5/3/14/SB	140	8.20
28.	1.5/3/14/AW	150	8.79
29.	1.5/6/14/SB	160	9.37
30.	1.5/6/14/AW	140	8.20
31.	1.5/9/14/SB	150	8.79
32.	1.5/9/14/AW	140	8.20
33.	1.5/0/21/SB	200	11.72
34.	1.5/0/21/AW	180	10.55
35.	1.5/3/21/SB	165	9.67
36.	1.5/3/21/AW	150	8.79
37.	1.5/6/21/SB	160	9.37
38.	1.5/6/21/AW	170	9.96
39.	1.5/9/21/SB	140	8.20
40.	1.5/9/21/AW	140	8.20
41.	1.5/0/28/SB	220	12.89
42.	1.5/0/28/AW	180	10.55
43.	1.5/3/28/SB	180	10.55

Contd....

Continued

44.	1.5/3/28/AW	160	9.37
45.	1.5/6/28/SB	150	8.79
46.	1.5/6/28/AW	130	7.62
47.	1.5/9/28/SB	135	7.91
48.	1.5/9/28/AW	135	7.91
49.	1.5/0/60/SB	180	10.55
50.	1.5/0/60/AW	160	9.37
51.	1.5/3/60/SB	150	8.79
52.	1.5/3/60/AW	130	7.62
53.	1.5/6/60/SB	145	8.49
54.	1.5/6/60/AW	135	7.91
55.	1.5/9/60/SB	120	7.03
56.	1.5/9/60/AW	130	7.62

TABLE 3.5 : FLEXURAL STRENGTH TEST RESULTS - 1:3 MIX

S. No.	Sample	First Crack Load (kg)	First Cracking Strength (MPa)
57.	3/0/1/SB	100	5.86
58.	3/0/1/AW	95	5.57
59.	3/3/1/SB	80	4.69
60.	3/3/1/AW	90	5.27
61.	3/6/1/SB	120	7.03
62.	3/6/1/AW	90	5.27
63.	3/9/1/SB	85	4.98
64.	3/9/1/AW	100	5.86
65.	3/0/3/SB	120	7.03
66.	3/0/3/AW	125	7.32
67.	3/3/3/SB	130	7.62
68.	3/3/3/AW	120	7.03
69.	3/6/3/SB	140	8.20
70.	3/6/3/AW	130	7.62
71.	3/9/3/SB	120	7.03
72.	3/9/3/AW	130	7.62
73.	3/0/7/SB	160	9.37
74.	3/0/7/AW	160	9.37
75.	3/3/7/SB	150	8.79
76.	3/3/7/AW	130	7.62
77.	3/6/7/SB	145	8.49

Contd...

Continued

78.	3/6/7/AW	160	9.37
79.	3/9/7/SB	140	8.20
80.	3/9/7/AW	135	7.91
81.	3/0/14/SB	185	10.84
82.	3/0/14/AW	165	9.67
83.	3/3/14/SB	155	9.08
84.	3/3/14/AW	150	8.79
85.	3/6/14/SB	135	7.91
86.	3/6/14/AW	140	8.20
87.	3/9/14/SB	140	8.20
88.	3/9/14/AW	145	8.49
89.	3/0/21/SB	170	9.96
90.	3/0/21/AW	150	8.79
91.	3/3/21/SB	145	8.49
92.	3/3/21/AW	130	7.62
93.	3/6/21/SB	140	8.20
94.	3/6/21/AW	135	7.91
95.	3/9/21/SB	130	7.62
96.	3/9/21/AW	130	7.62
97.	3/0/28/SB	165	9.67
98.	3/0/28/AW	155	9.08
99.	3/3/28/SB	150	8.79
100.	3/3/28/AW	135	7.91

Contd....

Continued

101. 3/6/28/SB	130	7.62
102. 3/6/28/AW	125	7.32
103. 3/9/28/SB	130	7.62
104. 3/9/28/AW	145	8.49
105. 3/0/60/SB	150	8.79
106. 3/0/60/AW	120	7.03
107. 3/3/60/SB	140	8.20
108. 3/3/60/AW	135	7.91
109. 3/6/60/SB	140	8.20
110. 3/6/60/AW	125	7.32
111. 3/9/60/SB	120	7.03
112. 3/9/60/AW	110	6.44

TABLE 3.6 : LOAD Vs DEFLECTION (CENTRAL)

S.No.	LOAD (kg)	CENTRAL DEFLECTION (mm)		
		1.5/9/28/AW-2	3/0/7/SB-1	3/0/14/AW-2
1.	20	0.08	0.26	0.20
2.	40	0.19	0.44	0.42
3.	60	0.31	0.65	0.60
4.	80	0.40	1.04	0.81
5.	100	0.49	1.49	1.15
6.	120	0.58	2.00	1.60
7.	140	0.68	2.53	2.60
8.	150		2.88	3.30
9.	160	12.1		4.16
10.	170		14.33	
11.	180			17.1

TABLE 3.7 : BENDING STRESS Vs STAIN (TENSILE)

S. No.	BENDING STRESS (MPa)	MICROSTRAIN (με)				
		1.5/9/28/AW	3/0/7/SB	3/0/14/AW	3/3/14/SB	1.5/0/21/SB
1.	1.172	86	125	26	134	16
2.	2.344	100	264	82	215	72
3.	3.516	145	680	157	284	137
4.	4.688	192	1316	301	658	339
5.	5.86	231	2079	1197	1685	1331
6.	7.032	270	2980	2146	2599	2443
7.	8.204	341	3788	3637	3442	3688
8.	8.49	3619				
9.	8.79		4869			
10.	9.37			5597	4166	4748
11.	10.55					7106
12.	11.72					7229

TABLE 3.8 : SPONTANEOUS POTENTIAL TEST SCALE (in Calomel scale) FOR 1:1.5 MIX

S.No.	Period of Corrosion (days)	Spontaneous Potential (mV_{see}) 0%	3%	6%	9%
(a) Submerged Conditions :					
1.	1	375	410	365	445
2.	3	431	627	438	465
3.	7	470	589	502	470
4.	14	560	510	480	560
5.	21	493	445	460	425
6.	28	693	910	770	516
7.	60	477	452	317	286
(b) Alternate Wetting and Drying Conditions :					
1.	1	380	476	475	405
2.	3	439	560	590	501
3.	7	551	462	612	612
4.	14	496	480	539	570
5.	21	477	424	525	929
6.	28	518	960	488	650
7.	60	454	561	407	517

TABLE 3.9 : SPONTANEOUS POTENTIAL TEST SCALE (in Calomel scale) FOR 1:3 MIX

S.No.	Period of Corrosion (days)	Spontaneous Potential (mV_{see}) 0%	3%	6%	9%
(a) Submerged Conditions :					
1.	1	390	325	411	438
2.	3	448	478	481	504
3.	7	425	568	517	517
4.	14	486	540	445	700
5.	21	775	420	528	601
6.	28	618	450	477	627
7.	60	512	501	403	425
(b) Alternate Wetting and Drying Conditions :					
1.	1	401	375	421	368
2.	3	460	489	558	512
3.	7	450	530	521	502
4.	14	430	748	486	535
5.	21	504	530	490	570
6.	28	514	466	698	596
7.	60	450	410	380	350

TABLE 3.10 : CORROSION TEST RESULTS - 1:1.5 MIX

S. No.	SAMPLE	d (mm)	W_f (gm)	$(W_o - W_f)$ (mg)	t (days)	C_e (md)	C_r (mdd)
1.	1.5/0/1/SB	0.75	0.336109	0.016	1	0.7	0.7
2.	1.5/0/1/AW	0.75	0.336097	0.028	1	1.2	1.2
3.	1.5/3/1/SB	0.75	0.336052	0.073	1	3.1	3.1
4.	1.5/3/1/AW	0.749	0.336033	0.092	1	3.9	3.9
5.	1.5/6/1/SB	0.75	0.335988	0.137	1	5.8	5.8
6.	1.5/6/1/AW	0.749	0.335987	0.138	1	5.9	5.9
7.	1.5/9/1/SB	0.75	0.335930	0.195	1	8.3	8.3
8.	1.5/9/1/AW	0.75	0.335942	0.183	1	7.8	7.8
9.	1.5/0/3/SB	0.749	0.336000	0.125	3	5.3	1.77
10.	1.5/0/3/AW	0.749	0.335932	0.193	3	8.2	2.73
11.	1.5/3/3/SB	0.749	0.335800	0.325	3	13.8	4.61
12.	1.5/3/3/AW	0.748	0.335751	0.374	3	15.9	5.30
13.	1.5/6/3/SB	0.748	0.335744	0.381	3	16.2	5.40
14.	1.5/6/3/AW	0.748	0.335658	0.467	3	19.9	6.63
15.	1.5/9/3/SB	0.746	0.335625	0.499	3	21.3	7.10
16.	1.5/9/3/AW	0.748	0.335606	0.519	3	22.1	7.37
17.	1.5/0/7/SB	0.749	0.335706	0.419	7	17.8	2.54
18.	1.5/0/7/AW	0.749	0.335596	0.529	7	22.5	3.21
19.	1.5/3/7/SB	0.746	0.335232	0.893	7	38.1	5.44
20.	1.5/3/7/AW	0.747	0.335086	1.039	7	44.3	6.44

Contd....

Continued

21.	1.5/6/7/SB	0.748	0.334969	1.156	7	49.2	7.03
22.	1.5/6/7/AW	0.747	0.334802	1.323	7	56.4	8.06
23.	1.5/9/7/SB	0.745	0.334683	1.442	7	61.6	8.80
24.	1.5/9/7/AW	0.747	0.334525	1.600	7	68.2	9.74
25.	1.5/0/14/SB	0.746	0.334670	1.455	14	62.1	4.44
26.	1.5/0/14/AW	0.745	0.334452	1.673	14	71.5	5.11
27.	1.5/3/14/SB	0.745	0.334379	1.746	14	74.6	5.33
28.	1.5/3/14/AW	0.744	0.334251	1.874	14	80.2	5.73
29.	1.5/6/14/SB	0.744	0.334061	2.064	14	88.3	6.31
30.	1.5/6/14/AW	0.742	0.333936	2.189	14	93.9	6.71
31.	1.5/9/14/SB	0.743	0.333268	2.857	14	122.4	8.74
32.	1.5/9/14/AW	0.741	0.333059	3.066	14	131.7	9.41
33.	1.5/0/21/SB	0.743	0.334160	1.965	21	84.2	4.01
34.	1.5/0/21/AW	0.741	0.333883	2.242	21	96.3	4.59
35.	1.5/3/21/SB	0.742	0.333139	2.986	21	128.1	6.10
36.	1.5/3/21/AW	0.740	0.333882	2.243	21	96.5	4.60
37.	1.5/6/21/SB	0.739	0.332227	3.898	21	167.9	7.80
38.	1.5/6/21/AW	0.740	0.332064	4.061	21	174.7	8.32
39.	1.5/9/21/SB	0.739	0.331368	4.757	21	204.9	9.76
40.	1.5/9/21/AW	0.738	0.330732	5.393	21	232.6	11.08
41.	1.5/0/28/SB	0.739	0.333065	3.060	28	131.8	4.71
42.	1.5/0/28/AW	0.736	0.332874	3.251	28	140.6	5.02
43.	1.5/3/28/SB	0.738	0.331854	4.271	28	184.2	6.58

Contd....

Continued

44.	1.5/3/28/AW	0.736	0.331586	4.539	28	196.3	7.01
45.	1.5/6/28/SB	0.735	0.330828	5.297	28	229.4	8.19
46.	1.5/6/28/AW	0.732	0.330427	5.698	28	247.8	8.85
47.	1.5/9/28/SB	0.731	0.329589	6.536	28	284.6	10.16
48.	1.5/9/28/AW	0.730	0.328711	7.414	28	323.3	11.55
49.	1.5/0/60/SB	0.729	0.330429	5.696	60	248.7	4.15
50.	1.5/0/60/AW	0.730	0.329106	7.019	60	297.9	4.97
51.	1.5/3/60/SB	0.729	0.328148	7.977	60	348.3	5.81
52.	1.5/3/60/AW	0.728	0.327496	8.629	60	377.3	6.29
53.	1.5/6/60/SB	0.729	0.324298	11.827	60	516.4	8.61
54.	1.5/6/60/AW	0,725	0.323744	12.383	60	543.6	9.06
55.	1.5/9/60/SB	0.727	0.319875	16.250	60	711.5	11.86
56.	1.5/9/60/AW	0.720	0.319633	16.492	60	729.1	12.15

NOTE :- (i) d = Diameter of the sample wire (reduced) (dm)

(ii) W_f = Net weight after corrosion (gm)

(iii) W_o = Original weight (gm) = 0.336125 gm

(iii) $W_o - W_f$ = Loss in weight (mg)

(iv) t = Period of corrosion (days)

(v) C_e = Extent of corrosion = $(W_o - W_f)/(\pi dL)$ (md)

(vi) C_r = Rate of corrosion = C_e/t (mdd)

(vii) L = Length of sample wire (dm) = 1 dm

TABLE 3.11 : CORROSION TEST RESULTS - 1:3 MIX

S. No.	SAMPLE	d (mm)	W_f (gm)	$(W_o - W_f)$ (mg)	t (days)	C_e (md)	C_r (mdd)
57.	3/0/1/SB	0.750	0.336106	0.019	1	0.8	0.8
58.	3/0/1/AW	0.750	0.336076	0.049	1	2.1	2.1
59.	3/3/1/SB	0.750	0.336059	0.066	1	2.8	2.8
60.	3/3/1/AW	0.750	0.336043	0.082	1	3.5	3.5
61.	3/6/1/SB	0.749	0.336012	0.113	1	4.8	4.8
62.	3/6/1/AW	0.750	0.336005	0,120	1	5.1	5.1
63.	3/9/1/SB	0.749	0.335946	0.179	1	7.6	7.6
64.	3/9/1/AW	0.750	0.335915	0.210	1	8.9	8.9
65.	3/0/3/SB	0.750	0.335998	0.127	3	5.4	1.8
66.	3/0/3/AW	0.749	0.335939	0.186	3	7.9	2.63
67.	3/3/3/SB	0.748	0.335862	0.263	3	11.2	3.73
68.	3/3/3/AW	0.748	0.335766	0.359	3	15.3	5.1
69.	3/6/3/SB	0.748	0.335728	0.397	3	16.9	5.63
70.	3/6/3/AW	0.747	0.335656	0.469	3	20.0	6.67
71.	3/9/3/SB	0.748	0.335594	0.531	3	22.6	7.53
72.	3/9/3/AW	0.746	0.335537	0.588	3	25.1	8.37
73.	3/0/7/SB	0.749	0.335730	0.395	7	16.8	2.4
74.	3/0/7/AW	0.749	0.335563	0.562	7	23.9	3.41
75.	3/3/7/SB	0.748	0.335274	0.851	7	36.2	5.17
76.	3/3/7/AW	0.748	0.335194	0.931	7	39.6	5.66

Contd....

Continued

77.	3/6/7/SB	0.748	0.334896	1.229	7	52.3	7.47
78.	3/6/7/AW	0.748	0.334844	1.281	7	54.5	7.79
79.	3/9/7/SB	0.746	0.334475	1.650	7	70.4	10.06
80.	3/9/7/AW	0.747	0.334607	1.518	7	64.7	9.24
81.	3/0/14/SB	0.746	0.334637	1.488	14	63.5	4.54
82.	3/0/14/AW	0.746	0.334438	1.687	14	72.0	5.14
83.	3/3/14/SB	0.744	0.334206	1.919	14	82.1	5.86
84.	3/3/14/AW	0.743	0.334099	2.026	14	86.8	6.20
85.	3/6/14/SB	0.741	0.333560	2.565	14	110.2	7.87
86.	3/6/14/AW	0.740	0.333256	2.869	14	123.4	8.81
87.	3/9/14/SB	0.738	0.332840	3.285	14	141.7	10.12
88.	3/9/14/AW	0.738	0.332364	3.761	14	162.2	11.59
89.	3/0/21/SB	0.740	0.333949	2.176	21	93.6	4.46
90.	3/0/21/AW	0.739	0.333773	2.352	21	101.3	4.82
91.	3/3/21/SB	0.738	0.332909	3.216	21	138.7	6.60
92.	3/3/21/AW	0.737	0.332803	3.322	21	142.5	6.83
93.	3/6/21/SB	0.737	0.331925	4.200	21	181.4	8.64
94.	3/6/21/AW	0.736	0.331704	4.421	21	191.2	9.10
95.	3/9/21/SB	0.735	0.330685	5.440	21	235.6	11.22
96.	3/9/21/AW	0.730	0.328628	7.497	21	326.9	15.57
97.	3/0/28/SB	0.736	0.332826	3.299	28	142.7	5.10
98.	3/0/28/AW	0.735	0.332440	3.685	28	159.6	5.70
99.	3/3/28/SB	0.734	0.331483	4.642	28	201.3	7.19

Contd....

Continued

100. 3/3/28/AW	0.735	0.332013	4.112	28	178.1	6.36
101. 3/6/28/SB	0.731	0.330090	6.035	28	262.8	9.39
102. 3/6/28/AW	0.730	0.329887	6.238	28	272.0	9.71
103. 3/9/28/SB	0.728	0.328614	7.511	28	328.4	11.73
104. 3/9/28/AW	0.728	0.327029	9.096	28	397.7	14.2
105. 3/0/60/SB	0.729	0.329326	6.799	60	296.9	4.95
106. 3/0/60/AW	0.728	0.328866	7.259	60	317.4	5.29
107. 3/3/60/SB	0.724	0.326886	9.239	60	406.2	6.77
108. 3/3/60/AW	0.726	0.326767	9.358	60	410.3	6.84
109. 3/6/60/SB	0.724	0.324220	12.703	60	558.5	9.31
110. 3/6/60/AW	0.724	0.323577	12.548	60	551.7	9.19
111. 3/9/60/SB	0.727	0.320288	15.837	60	693.4	11.56
112. 3/9/60/AW	0.700	0.319476	16.649	60	757.1	12.62

NOTE :- (i) d = Diameter of the sample wire (reduced) (dm)

(ii) W_f = Net weight after corrosion (gm)

(iii) W_o = Original weight (gm) = 0.336125 gm

(iii) $W_o - W_f$ = Loss in weight (mg)

(iv) t = Period of corrosion (days)

(v) C_e = Extent of corrosion = $(W_o - W_f)/(\pi dL)$ (md)

(vi) C_r = Rate of corrosion = C_e/t (mdd)

(vii) L = Length of sample wire (dm) = 1 dm

CHAPTER - IV

DISCUSSION OF RESULTS

4.1 GENERAL

The various tests conducted on the specimens are listed in the section 3.5 .The data obtained from the tests have been presented in the section 3.6. Within the limited scope of the experiments conducted in short duration of time, the results obtained have been analyzed and discussed in this chapter. The amount and rate of corrosion could not be varied in a controlled manner and, as such, these are being reported as influenced by sodium chloride concentrations, the mortar mix proportions and the duration of corrosion. The loss of flexural strength of the composite due to different amounts of corrosion is presented as the main finding of this study.

4.2 ANALYSIS OF RESULTS

4.2.1 First Crack Load vs Time

The plots of the first crack stress vs period of corrosion for 1:1.5 and 1:3 mortars under submerged and alternate wetting and drying conditions are given in Figs.4.1 to 4.4.

(i) BEHAVIOUR UNDER PLAIN WATER CURING

Under submerged conditions, the first cracking stress reaches a peak value at 28 days and between 14 to 21 days for 1:1.5 and 1:3 mixes respectively. The peak is followed by a slight decrease in the strength with time, which is about 10% for both the mixes.

Under alternate wetting and drying conditions, the peak values obtained are about 85-90% of the peaks obtained under submerged conditions. The peaks correspond to 21 day period of corrosion for 1:1.5 mix and to 14 days for 1:3 mix. The final decrease in the crack strength

as compared to the peak value is 14% and 24% for 1:1.5 and 1:3 mix proportions respectively .

(ii) BEHAVIOUR UNDER SALT SOLUTION CURING

For the case of accelerated corrosion, the specimens of 1:1.5 mix, cured under submerged conditions, showed the reduction of peaks by about 20-30% corresponding to 21-28 days, 14-21 days and 7-14 days for 3%, 6% and 9% salt concentrations respectively, as compared to the peak obtained under plain water curing. Under similar conditions, the specimens of 1:3 mix showed the corresponding reductions from 15-25% occurring at 14, 7 and between 7-14 days respectively for 3%, 6% and 9% solutions. The final decrease in the crack strengths as compared to the peak values after 28 days age are about 10-20% for 1:1.5 mix and about 9-15% for 1:3 mix.

Comparing the crack strength on similar lines for alternate wetting and drying conditions, the peak reductions are about 15-20% and the peaks correspond to 21, 14 and between 7-14 days for 3%, 6% and 9% solutions respectively for 1:1.5 mix and reduced by about 10-12% at 7-14 days for the 1:3 mix.

The initial increase in the crack strength is due to the gain in tensile strength of the mortar due to normal hydration reactions (refer Fig.4.5, curve A) . The presence of salt ions causes loss in strength due to corrosion at a rate that increases slightly with time (curve B) and thus the resulting curve (curve C) has a peak value at a point "a" where the two curves (A & B) intersect. Higher is the salt concentration, faster is the rate of corrosion and hence the loss in strength overtakes the gain due to mortar hardening in a shorter time period, resulting in lower peaks at early periods.

Thus the cracking strength showed a tendency of

stabilizing after an initial gain over the short period of time. According to the trends shown, it may tend towards a nearly constant value on long term basis. The final strengths tend to be stabilistic after 60 days at values 85-90% of the peak values in the case of plain water curing and at about 80-85% for accelerated curing under submerged conditions. For alternate wetting and drying conditions, under plain and salt water curing, the stabilization occurs at values 75-85% of the peak strengths. Similar indications are obtained from cracking strength vs C_e curves (Figs. 4.5 to 4.8).

Thus, to be on a safer side, it is advisable to take the design strength of ferrocement as 70% of the peak values at 28 days age.

4.2.2 First Crack Load vs C_e

The first cracking stress are plotted against extent of corrosion in Figs.4.6 to 4.9. The curves typically show a steeply rising limb and a peak beyond which the stress goes on decreasing with an increase in the extent of corrosion .

(i) UNDER SUBMERGED CONDITIONS :

The peak stress value is about twice the original stress value corresponding to a C_e value ranging between 80-120 md for the submerged conditions. The cracking strength decreased by about 25% as compared to the peak value when C_e reached a value as high as 700 md. However even at such a high C_e, the cracking stress was about 40% higher than the original value at very low C_e values.

(ii) UNDER ALTERNATE WETTING & DRYING CONDITIONS :

Under alternate wetting and drying conditions, the peak value was about 1.6 times the original value, occurring between 80 to 120 md. The decrease in the cracking strength was about 25-30% at C_e of 730 md. The final strength values were 22% and 15% higher than the

original strengths for 1:1.5 and 1:3 mortar mixes respectively.

The initial gain in the first cracking stress may be explained by the filling in of the pores of the hardened mortar by the products of corrosion which may seal off any continuous pore cavities in the matrix. Unless the volume of corrosion products becomes very high resulting in internal disintegration and continuity of micro cracks within the matrix, the gain in strength is not lost completely with increasing corrosion. The results also show that the above behaviour is independent of the conditions of the environment responsible for causing corrosion. The pH probably dropped from 13.0 to around 10.5 to 11.0 which marks the lower limit of the passive region in the Pourbaix diagram (refer Fig. 2.2)

Thus the corroding influences have little effect on the cracking strength of the composite i.e. the effect of cumulative corrosion does not result in any appreciable loss in cracking strength unless md assumes a very high value. The strength stabilizes at around 75-80% of the peak value obtained with plain water curing. The same results have been reflected in the variation of C_e vs time. And hence it can be conclusively said that the strength design values should be reduced by 30% to be on a conservative side with respect to corrosion.

4.2.3 Midspan Deflections

Typical load-deflection curves for three specimens are given in Fig.4.10 . The curves generally consisted of three distinct stages : (i) a steep linear portion before cracking of mortar, (ii) after the first cracking but before yielding of mesh ; and (iii) after yielding of meshes when the slope becomes almost parallel to the deflection axis. The first crack and yield loads were about 35% and 80% of the ultimate loads respectively. The average deflection at the first

crack load was span/420 and at the yield of mesh, span/100. Large deflections, even upto a value of span/20 have been taken by the samples at the ultimate load. According to the maximum allowable deflections specified by IS:456-78 as span/250, the load factors are found to lie in the range of 1.59 to 1.97. Therefore, a load factor of 1.5 may safely be adopted for designs based on the deflection criteria only.

The specimen 1.5/9/28/AW-2 was an exception to the general trend and showed a bilinear curve, with a steep initial linear portion upto the first crack value beyond which the curve was almost a horizontal line. It showed a load factor of 1.13 which is very low compared to the other specimens. Such a behaviour may be due to the loss in the yield strength of the meshes due to excessive corrosion (323.3md) so that the meshes yield immediately after the cracking of mortar. No sample exhibiting a higher corrosion than 323 md was tested for load-deflection behaviour.

Thus, excessive corrosion, resulting in lowering of the yield strength of the meshes, lowers the load factor and may reduce the normally trilinear load-deflection behaviour of the composite to a bilinear one. Very large deflections have been taken by the samples before failure.

4.2.4 Tensile Strain

Typical bending stress vs midspan tensile strain curves for five specimens - 3/0/7/SB-2, 3/0/14/AW-2, 1.5/0/21/SB-1, 3/3/14/SB-2 and 1.5/9/28/AW-2 are given in Fig.4.11 . The specimen 1.5/9/28/AW-2 showed a distinctly different behaviour from the general trend exhibited by the other four specimens. The four specimens showed three stages of behaviour : (i) the initial linear plot representing the elastic range with no crack formation. With a further increase of stress, ferrocement

becomes quasi-elastic, with micro cracks invisible to the naked eye. These two stages - the linear elastic and quasi-elastic constitute the practical elastic range of ferrocement; (ii) Cracked range - in which the curve deviates from linearity because of formation of cracks ; and (iii) Yield range - the curves become almost a straight line. In this stage, increasing mortar strains are caused by increasing width of cracks. The three stages have been marked in the case of specimen 3/3/14/SB-2 . For the purpose of illustration, the theoretical stress-strain curve of ferrocement in tension and the idealized curve in tension and compression are given in Figs.4.12 and 4.13 respectively. Thus, the plots of the four specimens follow the expected theoretical shape, with ultimate strains varying from (0.0042) to (0.0072) which are quiet high. Also, the modulus of elasticity of the composite increases slightly with age in its early life period and soon attains a constant value. The first crack loads occurred at about 25-40% of the ultimate loads.

Unlike the other four specimens, the specimen 1.5/9/28/AW-2 has exhibited a perfectly elastic behaviour till the first crack load and then as a perfectly plastic one (a bilinear curve) i.e. the intermediate cracked range is missing. The explanation is that the meshes yield in the specific case due to excessive corrosion immediately after the cracking of mortar. The specimen has shown a very high stiffness in the elastic range. The ultimate strain has reduced to 0.0036 in this case and the first crack load is about 87% of the ultimate load.

Thus excessive corrosion causes deviation in the stress-strain curve of the composite from a normal ideal one, by reducing the cracked range. It also causes reduction in the ultimate

strain value and thereby in the ductility or energy absorption capability.

4.2.5 Spontaneous (Half-Cell) Potential

The plots of variation of spontaneous potential with the period of corrosion are given in Figs.4.14 to 4.17 . According to the requirements of the ASTM C:876-91, the potential values have been compared on the copper-copper sulphate scale i.e. the CSE scale and it has been observed that the initial (1 day) electrical half cell potentials lie between -0.1 to -0.2 V with the final (60 day) values converging between 0 to -0.25 V. The trend showed that the values are likely to dip below -0.25 V at a very fast rate with further increase in period of corrosion since there is a sharp decrease in the values from 28 to 60 days. A somewhat similar behaviour has also been obtained by Tashiro and Ueoka (23) at 60 days age for ferrocement made with plain water, as in the present investigation.

The curves distinctly show the formation of two (and in a few cases, 3) peaks, the first being quite early (between 3-7 days) and the second one occurring anywhere between 14-28 days depending upon the mortar mix, the percentage of salt solution and the curing conditions. The peaks are seen to occur earlier for more aggressive environments. On comparison with the C_e vs time curves (Figs.4.1-4.4), it can be seen that the peak values of the spontaneous potential generally correspond to the peaks or the unusually high first cracking strength values as plotted against time, which thus substantiates the results obtained from the test.

The ASTM C:876-91 reports that a potential value higher than -0.2 Vcse signifies that no corrosion is occurring in the reinforcing steel. Potentials between -0.2 V and -0.35 V represent an

uncertain corrosion activity and values lower than -0.35 V (which is -0.3 V according to Tashiro and Ueoka (23)) show high corrosion activity. But these values are for an ungalvanized wire mesh. For a galvanized wire mesh, the values expected would be higher due to the protective effect of the Zinc layer and this has been obtained in this case, since the specimens giving high potential values (-0.1 to +0.1 V) are showing heavy corrosion. Thus, the limits of high corrosion activity would shift upwards by about 0.3 to 0.4 V due to the presence of the galvanizing layer. From the Pourbaix diagram (Fig.2.2) (24), it can be seen that the limit of potential values signifying corrosion varies according to the pH of the curing solution used, but generally a higher potential represents lower corrosion.

The formation of one or two valleys can be expected by the help of the corrosion phenomenon occurring within the sample. To start with, the pH of the sample drops (somewhat around 10) which ends the passive protection to the mesh. Then the corrosion process of the galvanizing layer starts with the formation of the white rust, which has shown a potential drop to around -0.1 V at 14-21 days. The final sharply receeding limb signifies the progressive corrosion of the steel of the wiremesh resulting in the formation of brown rust followed by black rust in severe cases. These results can be visibly seen in the Plates-3.3 to 3.16 .

Thus, the spontaneous potential test supports the strength results obtained and clearly shows the progress of corrosion in the samples. The corrosion of the galvanizing layer drops the potential value to around -0.1 V . The effect of the galvanizing layer makes the threshold limits of corrosion shift upwards by around 0.3 V . The sharply dropping potential in the final stages signify the progressive

nature of the corrosion of the iron.

Under submerged salt curing conditions (1:1.5 & 1:3 mixes) the spontaneous potential curves are depressed (down negatively) while in the alternate wetting and drying conditions they are pushed up positively. This is supported by the general corrosion theory that the extent of corrosion is smaller in the submerged state due to lack of oxygen and higher in AW state due to accumulation of salt ions.

A possible solution to the problem may be the use of a double galvanizing layer or stainless steel meshes which may be very costly. A cheaper alternative may be the use of 100-200ppm CrO_3 in the mixing water while preparing the mortar (11).

4.2.6 Extent and Rate of Corrosion

The plots of extent of corrosion (C_e) vs period of corrosion (t) are given in Figs.4.18 to 4.21 and those of the rate of corrosion (C_r) vs percentage of curing solution are given in Figs.4.22 to 4.25. The curves in Figs. 4.18 & 4.19 show that C_e increases significantly after a period of 7 days. The curve tends to be a straight line eventually. The effect of salt concentration on the extent of corrosion in the grades of mortars does not differ significantly.

(i) UNDER SUBMERGED CONDITIONS

Under submerged conditions, the C_e values for 3%, 6% & 9% solutions are respectively 1.4, 2.08 and 2.86 times the C_e value in plain water for the case of 1:1.5 mix. For 1:3 mortar, the corresponding values are 1.3, 1.88 and 2.34 respectively.

(ii) UNDER ALTERNATE WETTING & DRYING CONDITIONS

Under alternate wetting and drying conditions (Figs.4.20 & 4.21), the successive salt percentages causes the extent of corrosion to be 1.27, 1.82 and 2.45 times the md value in plain water for 1:1.5

mix and are 1.29, 1.74 and 2.38 times for 1:3 mix. The effect of alternate wetting and drying results in C_e values 10-20% higher than those obtained under submerged conditions and the effect is more pronounced in case of plain water curing.

The increase in the rate of corrosion (C_r) with increase in the concentration of salt solution is very evident from the C_r vs percentage salt solution graphs. The significant increase in C_r after 7 days has been quiet prominent in the case of 1:3-AW specimens (refer Fig.4.25) and in the case of specimens cured in potable water. Generally, for each concentration, the rate of corrosion at 60 days has increased by about 15-60% over the 7-day rates.

The reason for the above behaviour is the progressive nature of the corrosion phenomenon. The corrosion starts with the formation of oxide film which is adherent and impermeable in a passive environment. In an aggressive environment, the formed oxide is not adherent enough and occupies a volume 3 to 6 times larger than its original volume. This process produces pressure on the surrounding mortar causing micro cracking. Thus, the aggressive chloride ions get access more easily and the process of corrosion tends to be accelerated. Higher is the concentration of NaCl, more is the acceleration effect. Alternate wetting and drying also aggravates the corrosion and hence shows higher rates.

The studies indicate the necessity of using rich and dense mortars for ferrocement work i.e. 1:1.5 to 1:2 mix proportion with a water cement ratio preferably less than 0.45 . The study also clearly shows the need to use form or surface vibrators for compaction, wherever possible.

4.2.7 Visual Inspection

By inspecting the meshes extracted from the hardened mortar, it was observed that the corrosion damage was not uniform within a specimen, the mesh near the edges corroding more. This may be due to insufficient compaction at the edges or due to damaged edges resulting from handling of the specimens. Within a sample, various stages of corrosion could be observed. The initial stage of corrosion resulted in the production of a white corrosion product followed by a brown one. The colour of the corrosion product darkened with the progress of corrosion, starting from reddish brown to blackish brown. Specimens cured in plain water showed the production of only the white compound with specks of brown even after 60 days of curing. The magnified view also revealed excessive pitting and scaling of the wires in severe cases.

The white corrosion product is due to the corrosion of Zinc of the galvanizing layer of the wire mesh. The effect of Calcium hydroxide along with moisture can initiate a number of reactions giving Zinc hydroxide, Zinc oxide, Zincates, etc. , all white coloured compounds. One possible reaction giving Calcium zincate is :

$$Ca(OH)_2 + Zn \text{ -----> } CaZnO_2 + H_2$$

This reaction is not progressive and Calcium zincate protects the underlying metal by forming a passive layer, but only in the case of potable water. In the case of salt solutions, the galvanizing layer is not protective enough to prevent corrosion of steel and rusting progresses from one affected zone to the next, forming first the reddish brown corrosion product which is actually Fe_2O_3 , followed by the blackish brown compound which is Fe_3O_4 , signifying the highest degree of corrosion.

Thus, the side covers to the steel mesh should be

increased with better compaction. The galvanizing layer of the commercially available wiremesh is protective enough only in the case of potable water. For corrosive ion environments, it is suggested that 100 to 300 ppm Chromium trioxide (CrO_3) , which effectively passivates the zinc coating, may be added to the mixing water while preparing the mortar.

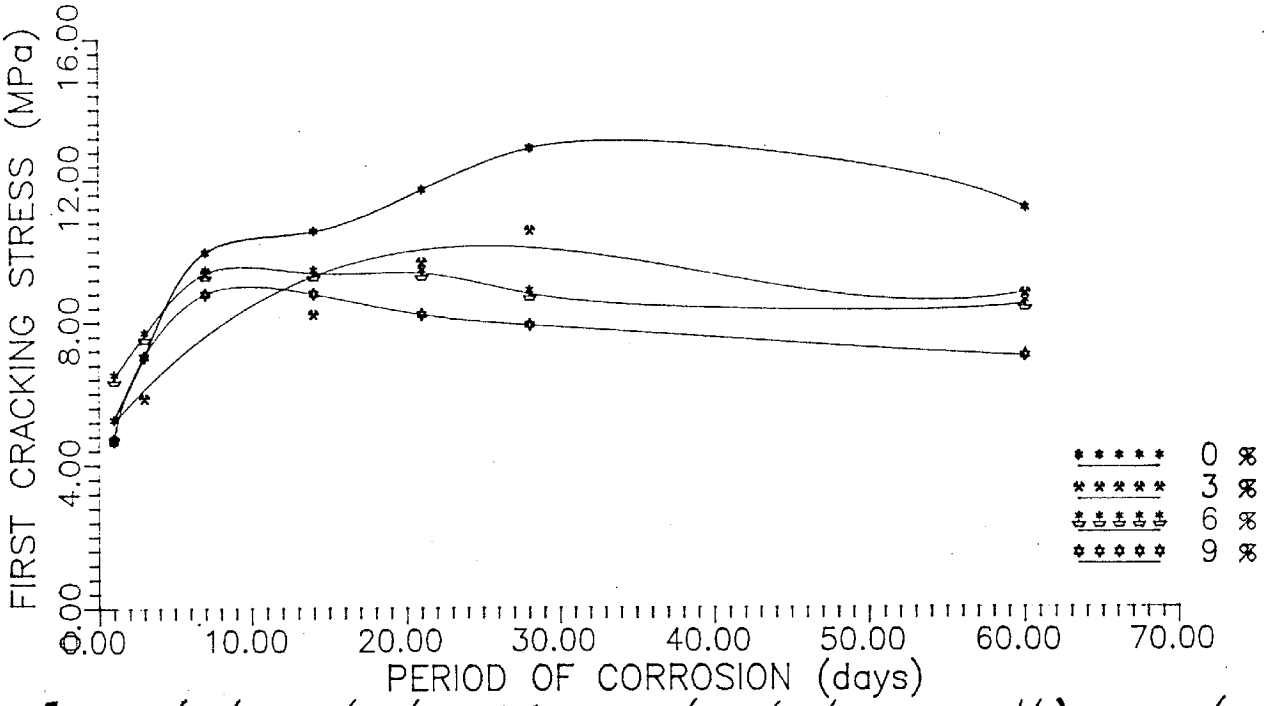

Fig 4.1 first crack stress (σ_{crb}) Vs. period of corrosion (t) curves for 1:1.5 mix (submerged conditions)

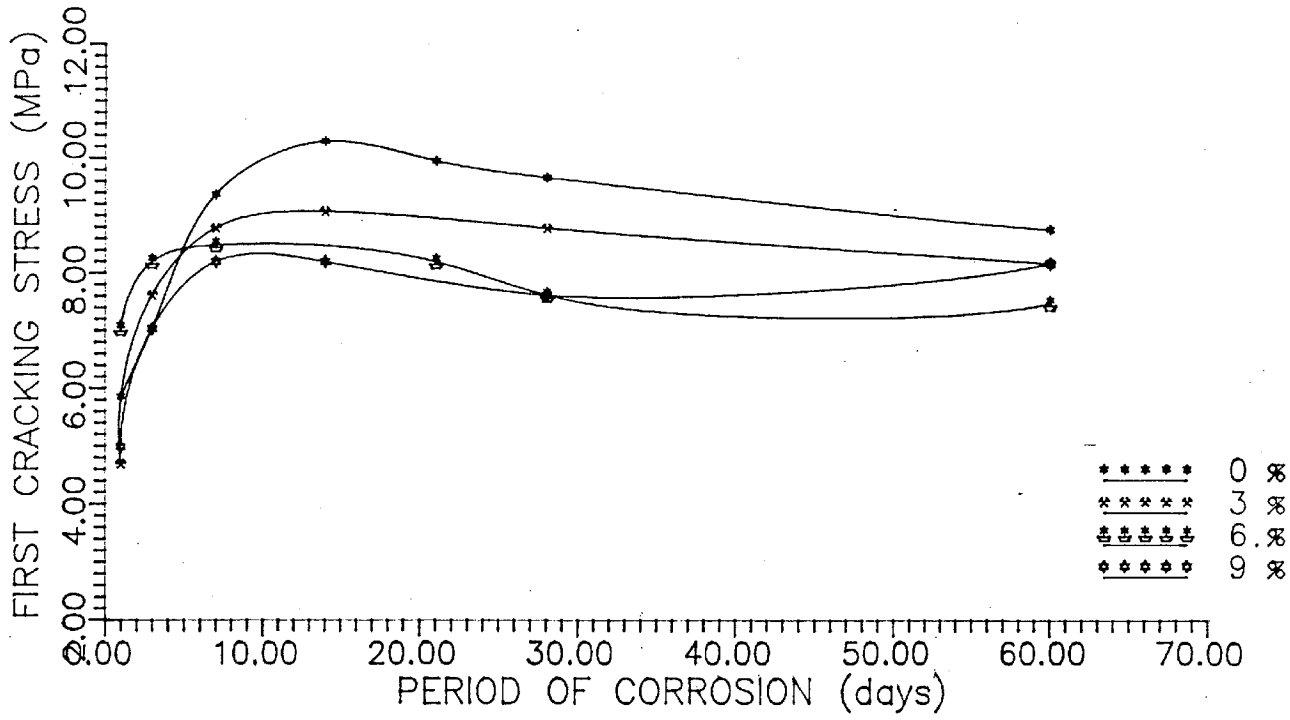

Fig 4·2 σ_{crb} Vs. t curves for 1:3 mix (submerged conditions)

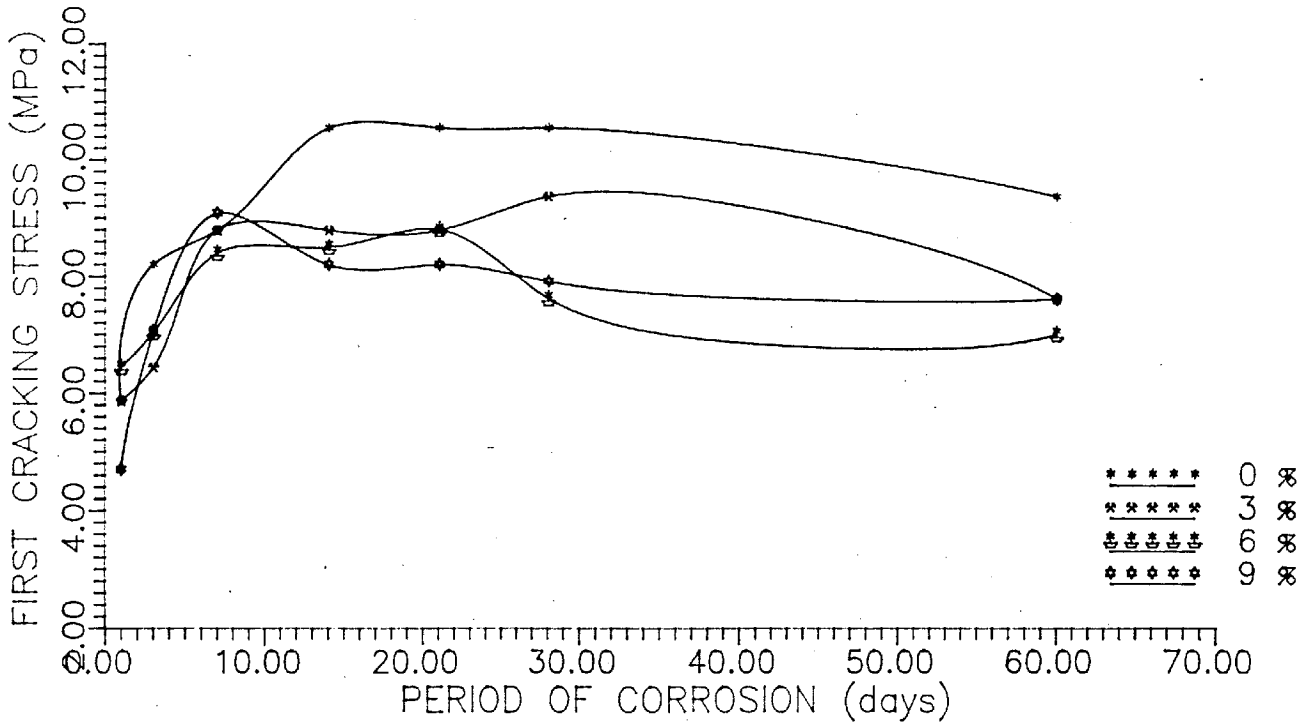

Fig 4.3 σ_{crb} Vs. t curves for 1:1.5 mix (alternate wetting & drying condition

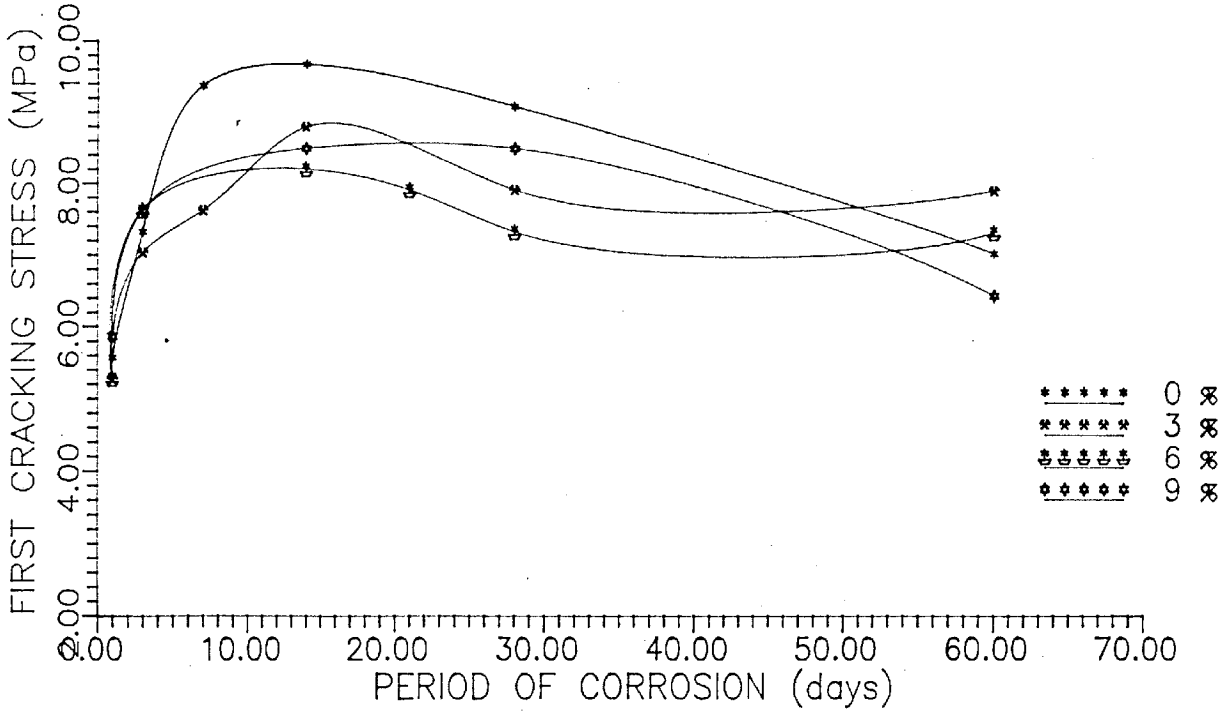

Fig 4.4 σ_{crb} Vs.t curves for 1:3 mix (alternate wetting & drying conditions)

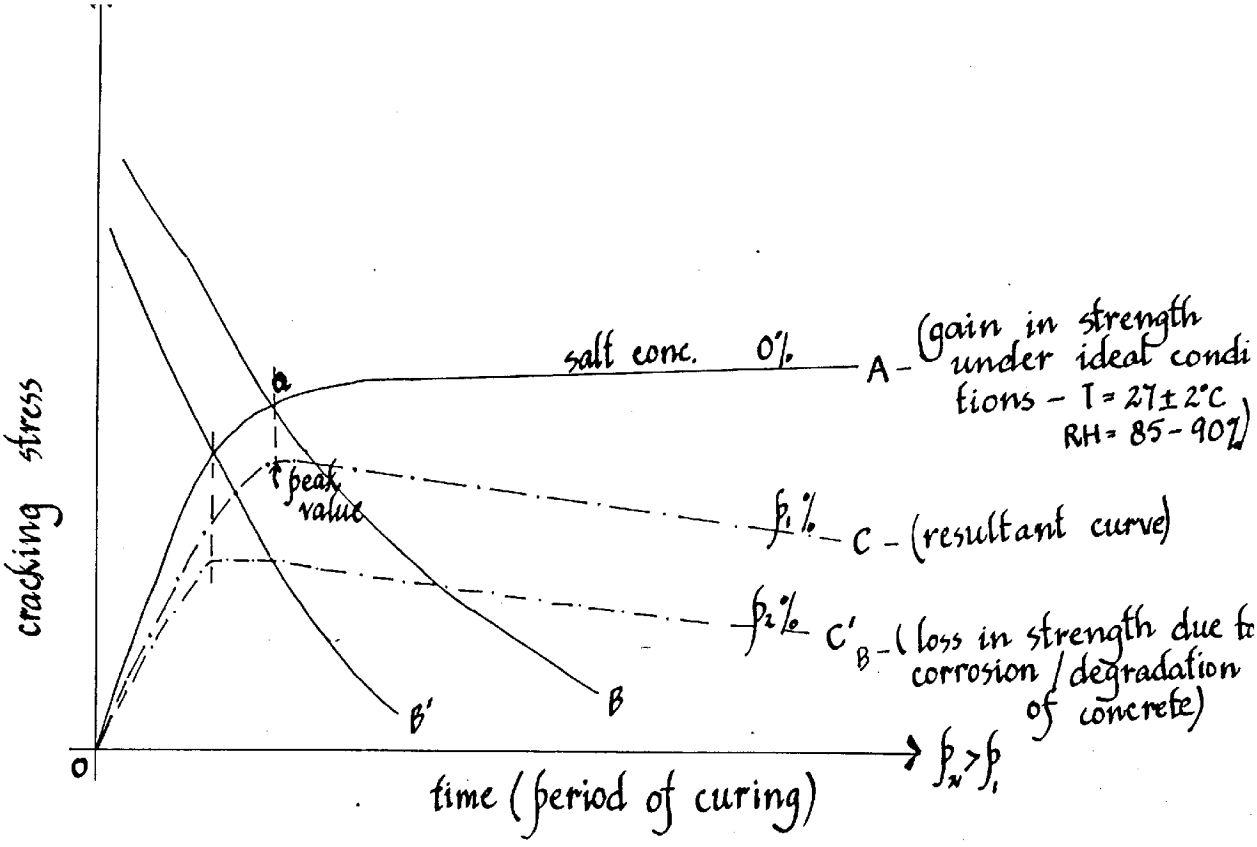

Fig 4.3 schematic cracking stress Vs. time (period of curing) curve

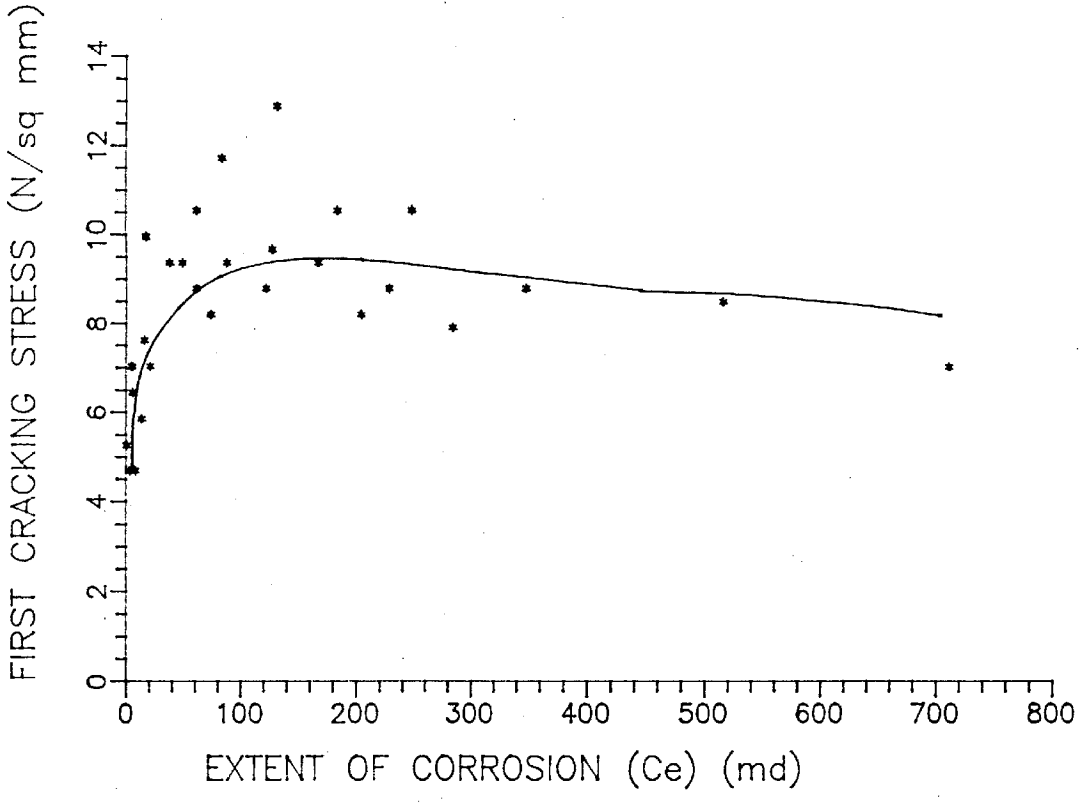

Fig 4.6 first cracking stress Vs Ce curve for 1:1:5 mix (submerged conditions)

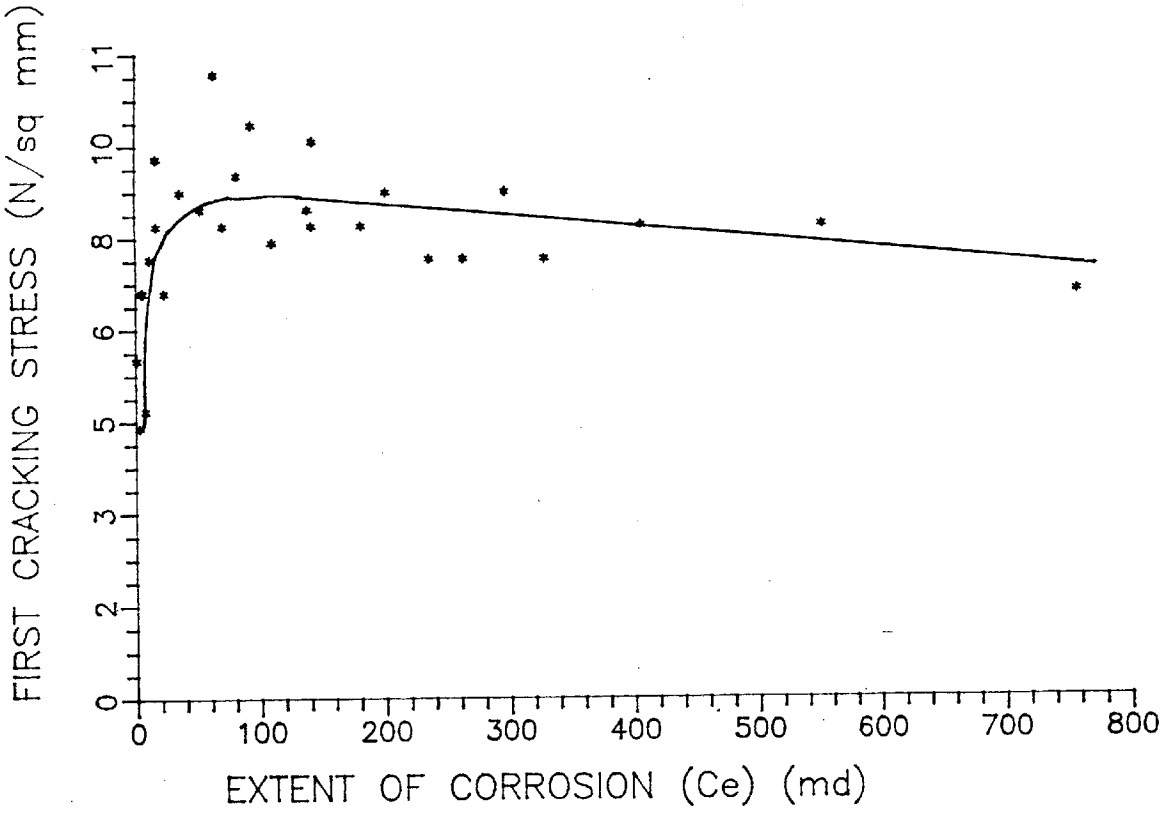

Fig 4.7 σ_{crb} Vs Ce curve for 1:3 mix (submerged conditions)

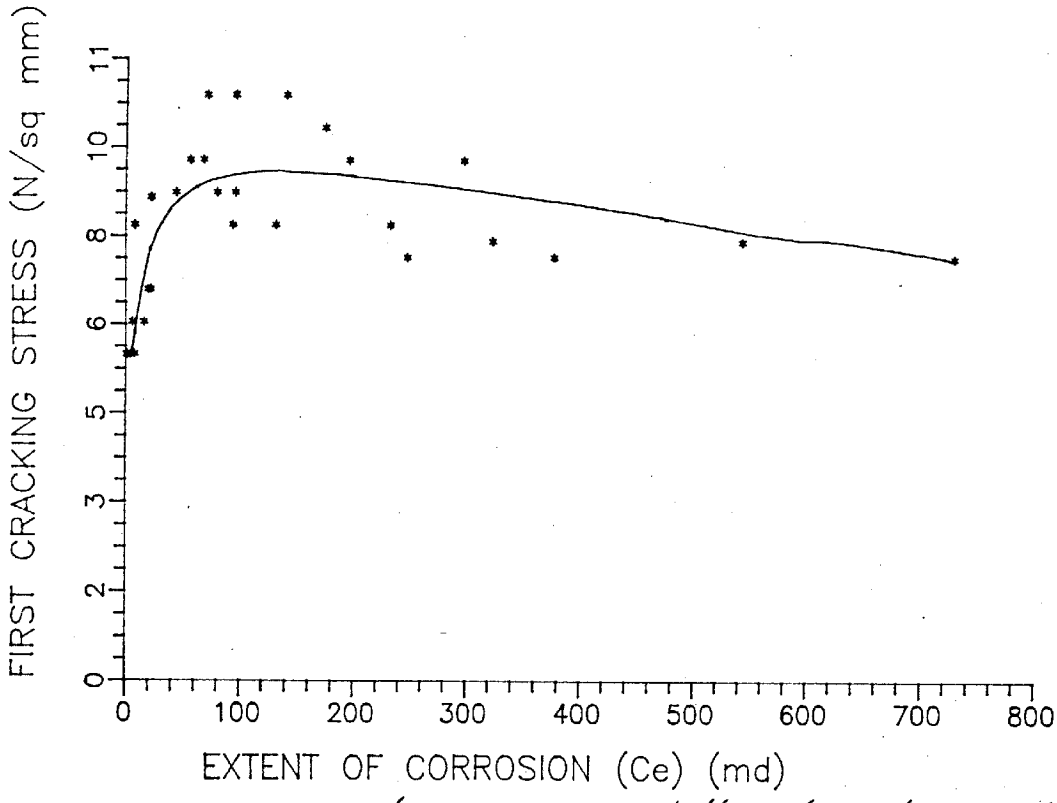

Fig 4.8 τ_{crb} Vs Ce curve for 1:1·5 mix (alternate wetting & drying conditions)

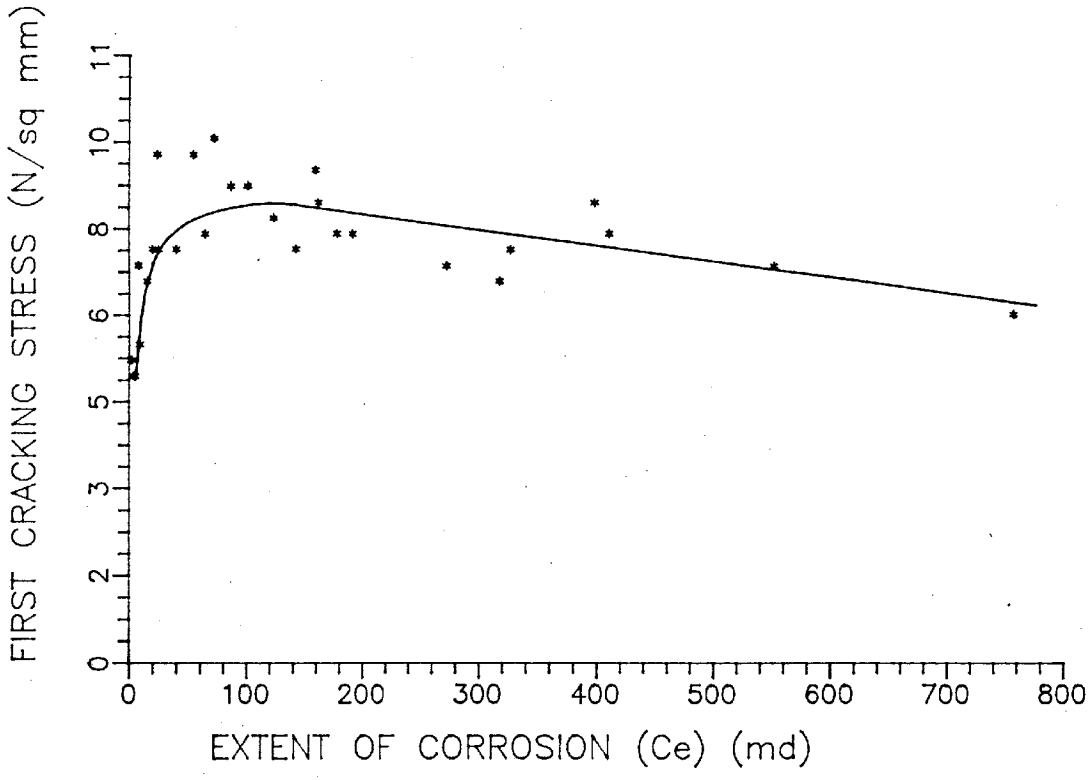

Fig 4.9 σ_{crb} Vs Ce curve for 1:3 mix (alternate wetting & drying conditions)

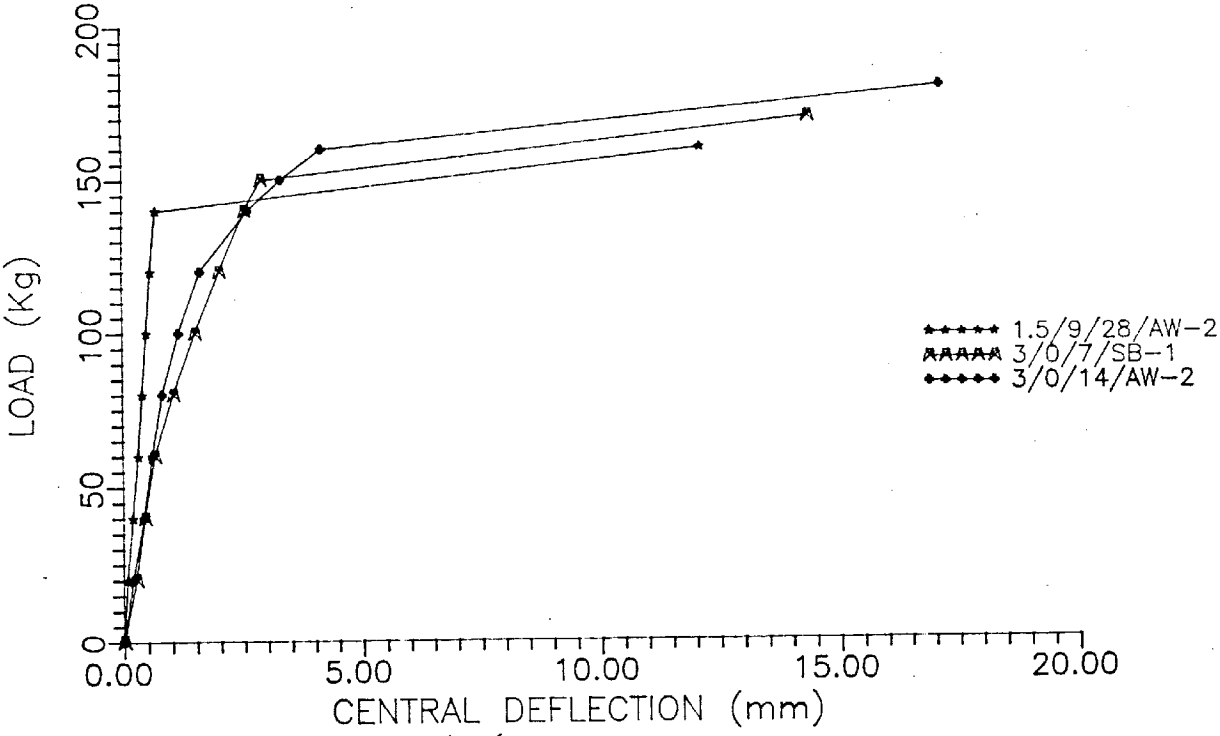

Fig 4·10 typical load - deflection curves

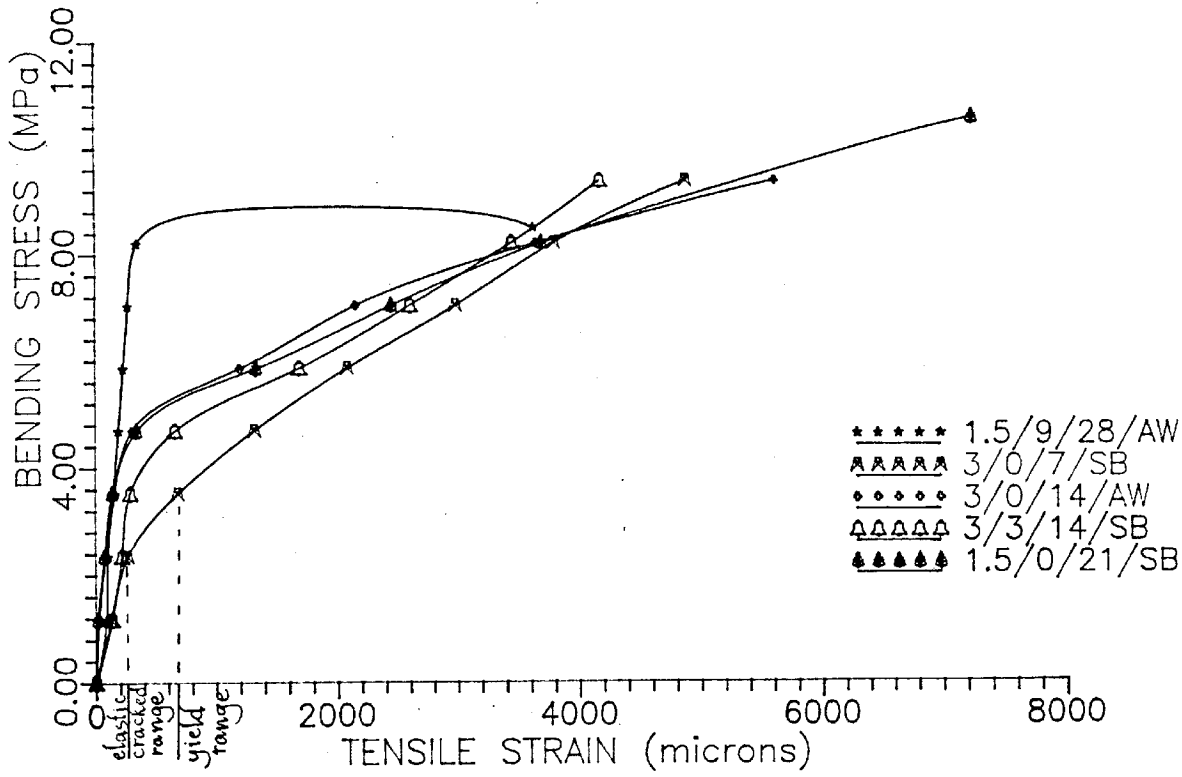

Fig 4·11 typical bending stress Vs. tensile strain curves

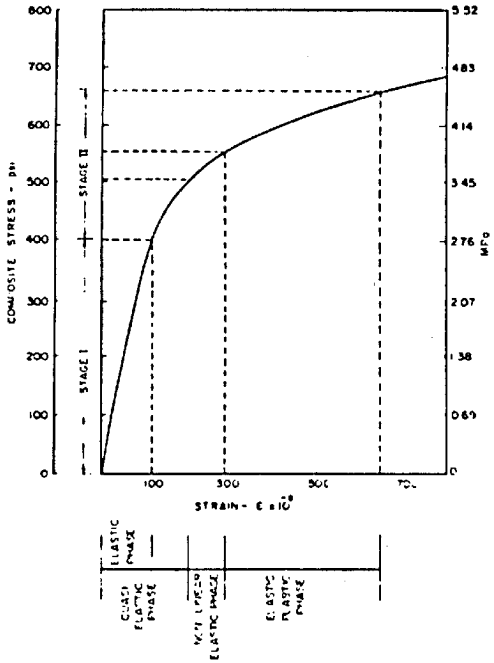

Fig 4·12 stress-strain curve of ferrocement in tension
*author [25]

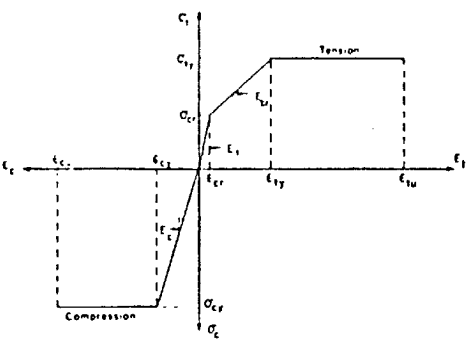

Fig 4·13 idealized stress-strain curve of ferrocement in tension and compression *author [25]

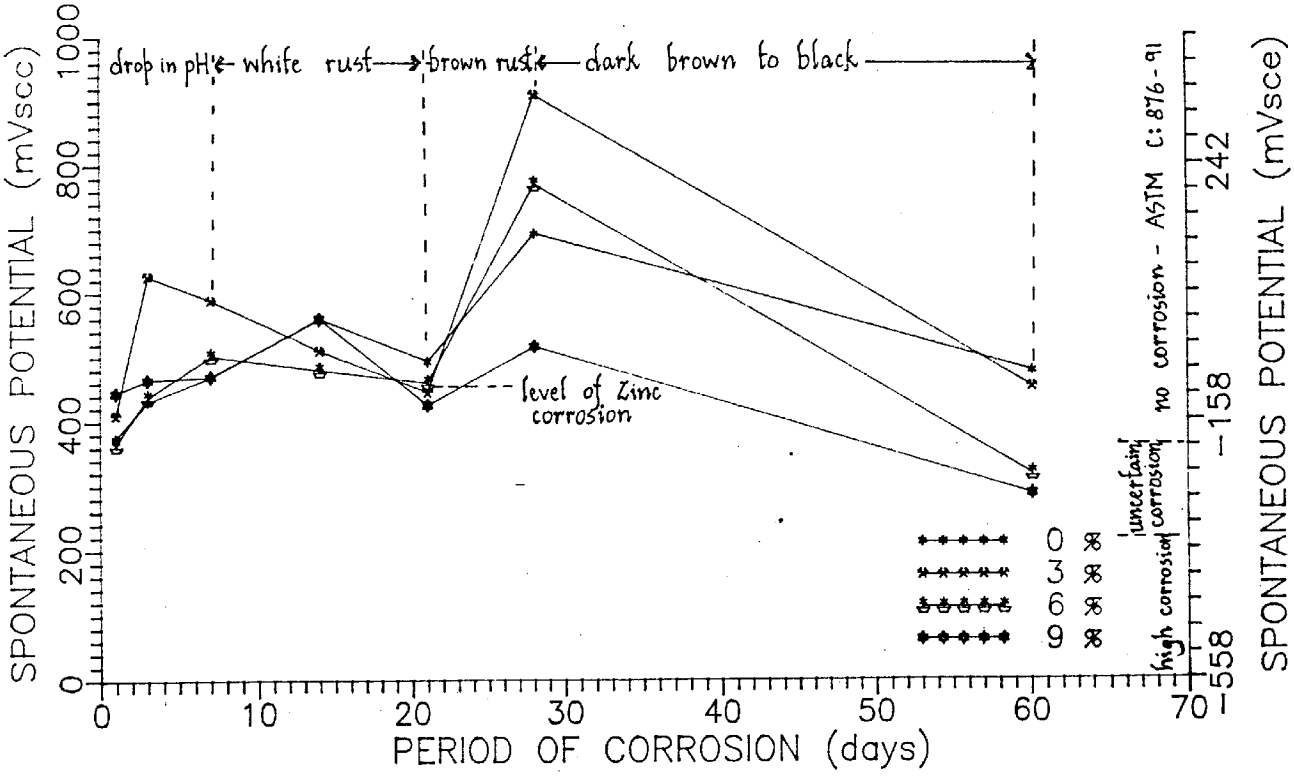

Fig 4·14 spontaneous potential Vs t - 1:1·5 mix (submerged conditions)

Fig 4.15 Spontaneous potential Vs t curves 1:3 mix (submerged conditions)

Fig 4.16 Spontaneous potential Vs. t curves for 1:1.5 mix (alt. wetting & dryi conditions)

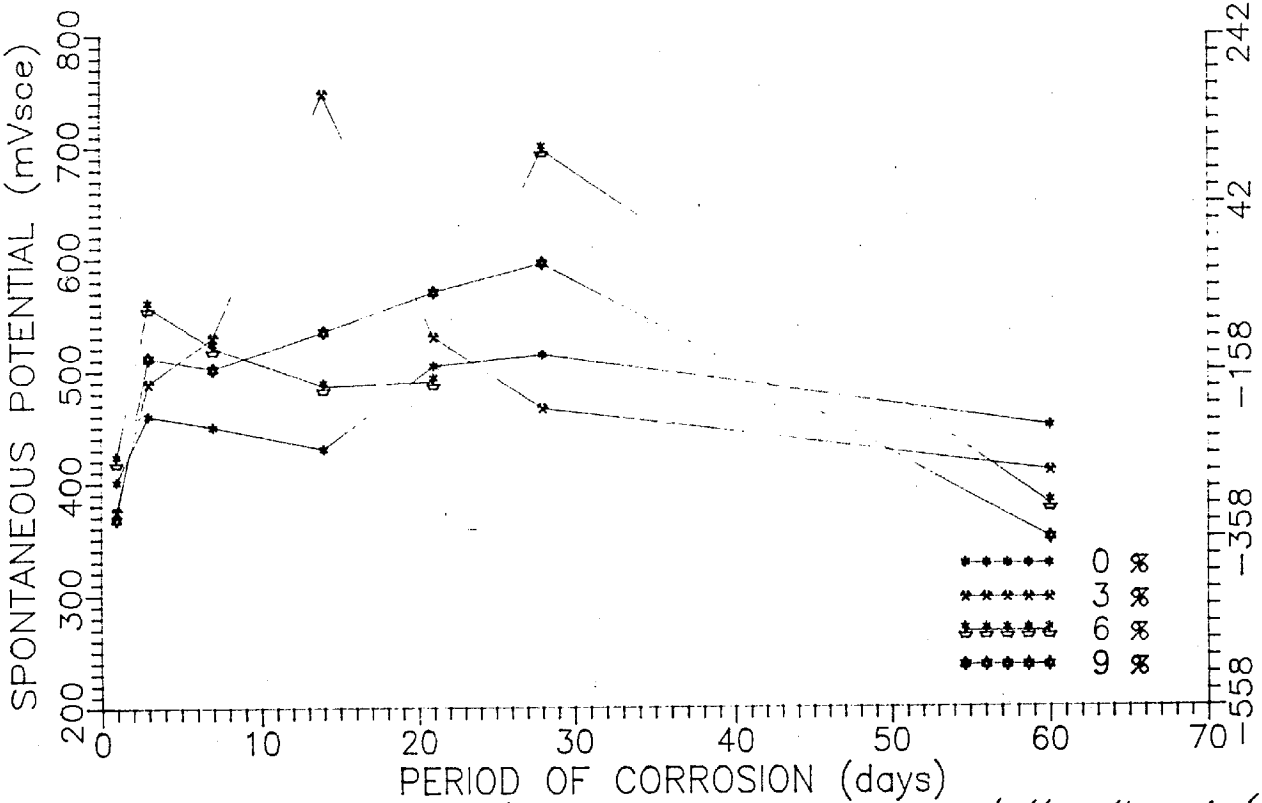

Fig 4.17 spontaneous potential Vs. t curves for 1:3 mix (alt. wetting & drying conditions)

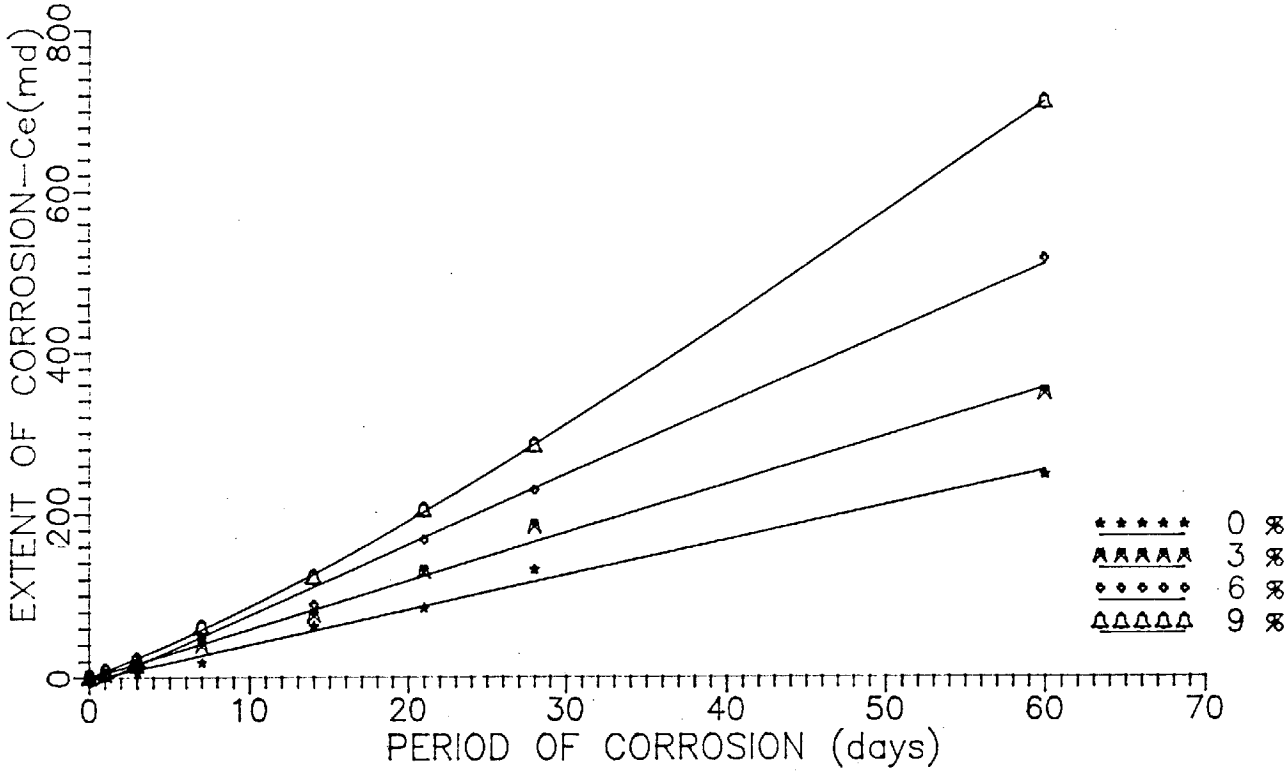

Fig 4·18 C_e Vs t curves for 1:1·5 mix (submerged conditions)

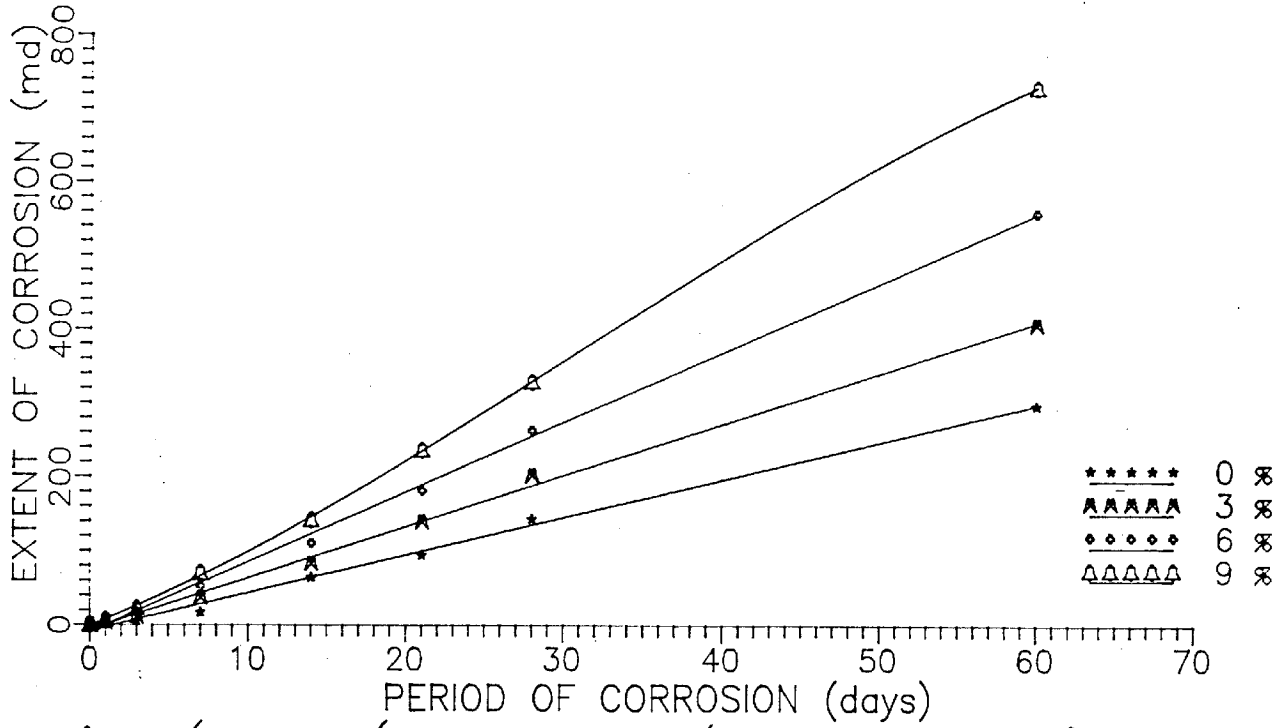

Fig 4.19 C_e Vs. t curves for 1:3 mix (submerged conditions)

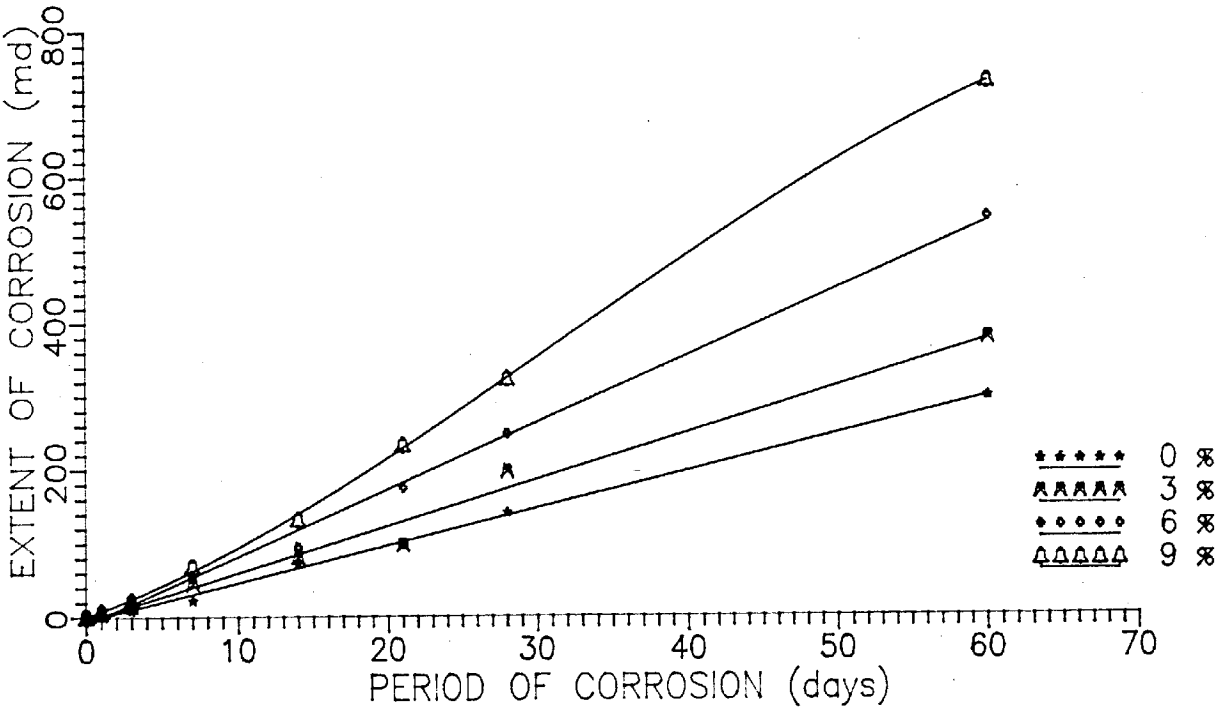

Fig 4.2 C_e Vs. t curves for 1:1.5 mix (alternate wetting & drying condition

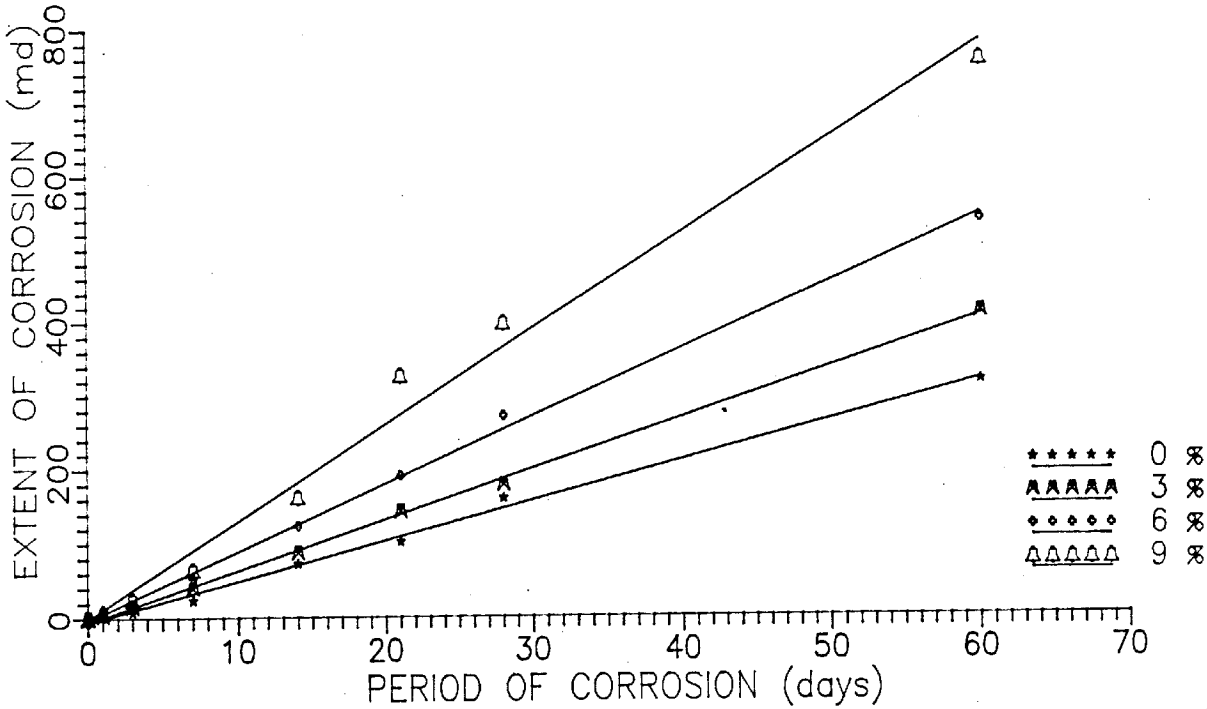

Fig 4.21 Ce Vs. t curves for 1:3 mix (alternate wetting & drying conditions)

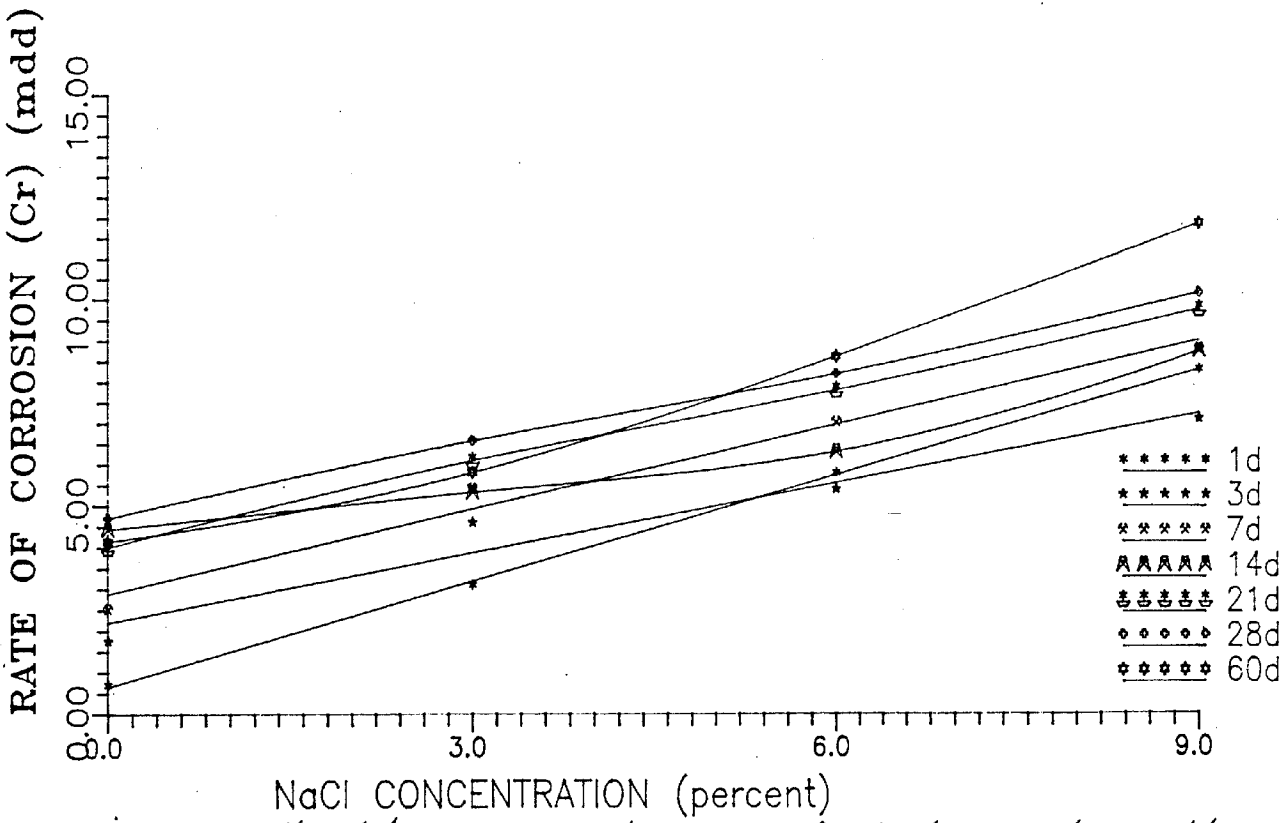

Fig 4.22 Cr Vs % salt solution curves (1:1.5 mix) (submerged conditions)

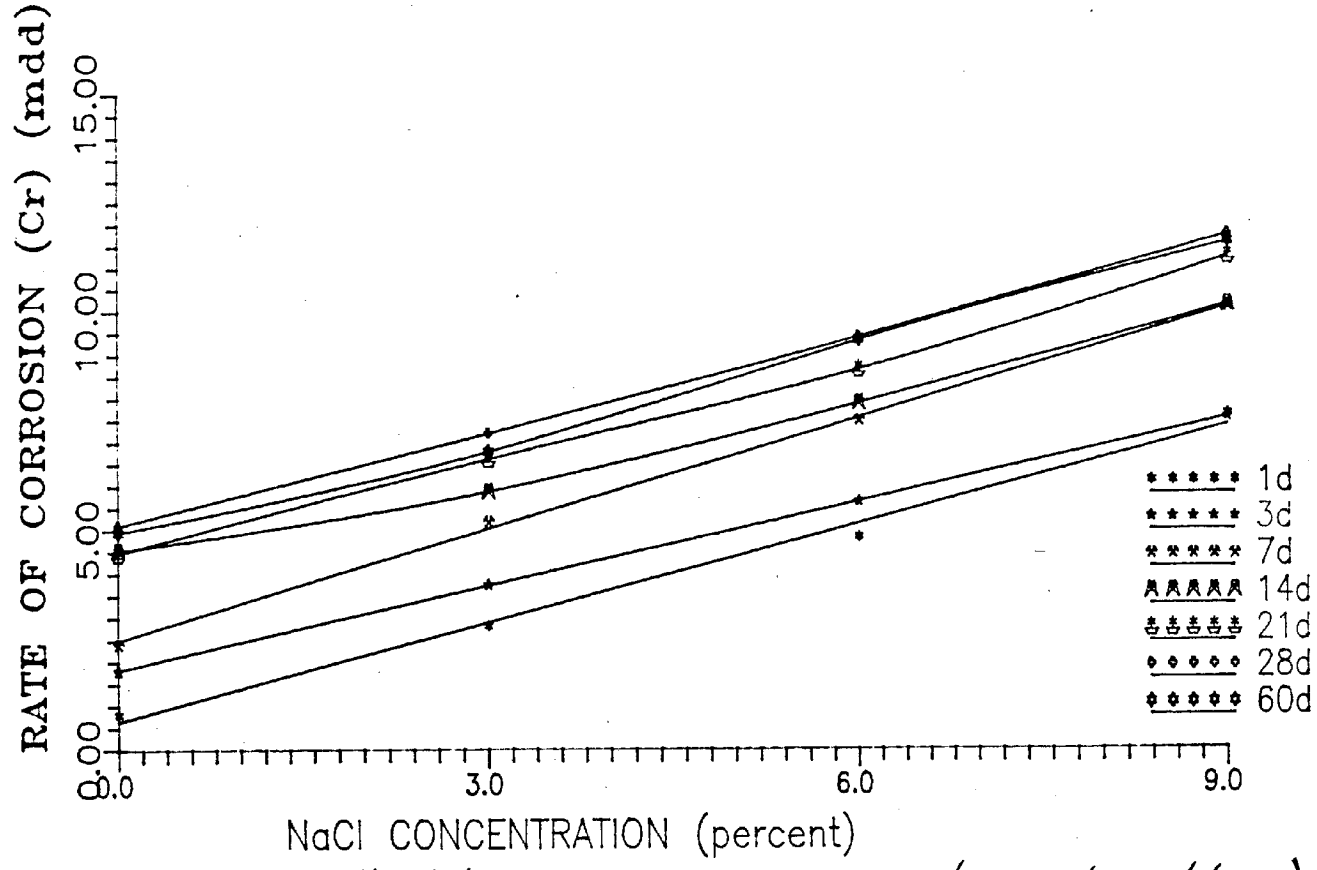

Fig 4.23 Cr Vs % salt solution curves 1:3 mix (submerged conditions)

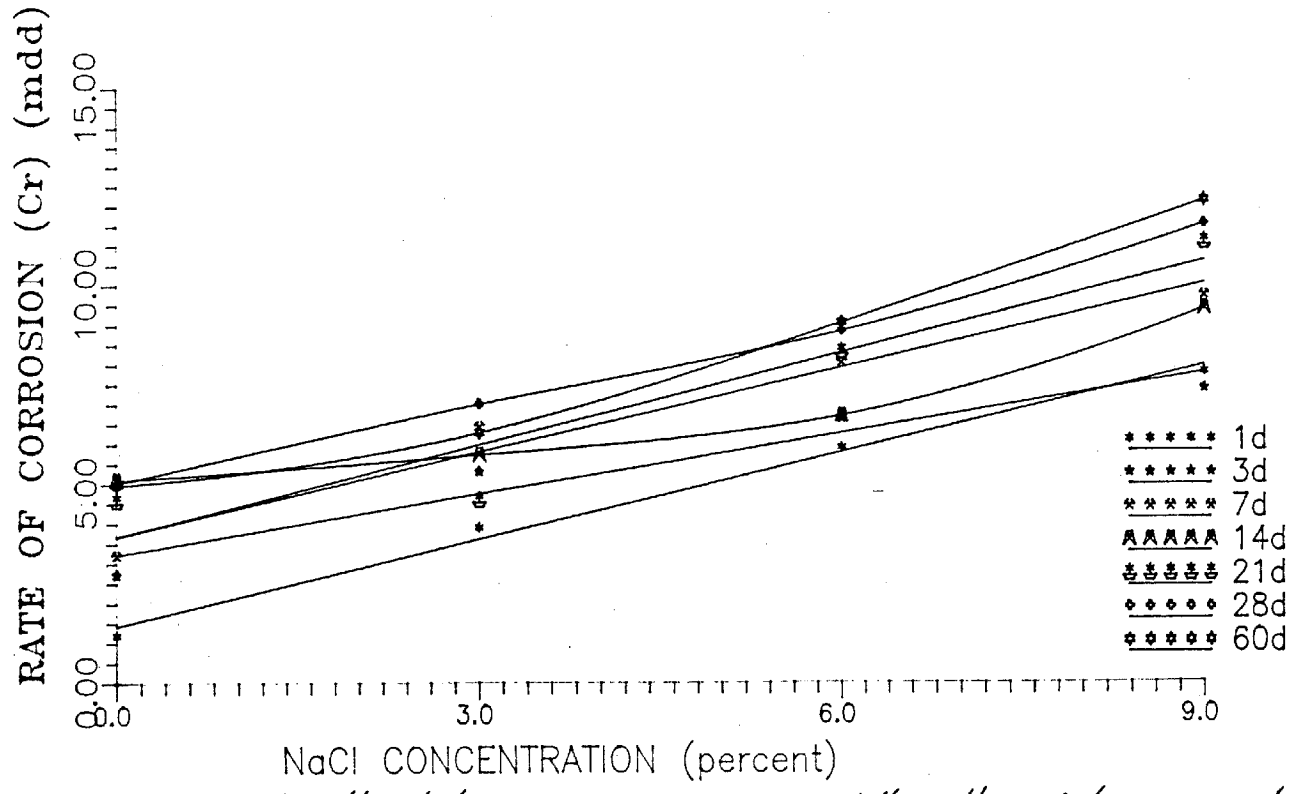

Fig 4.24 Cr Vs % salt solution curves 1:1·5 mix (alt. wetting & drying condition

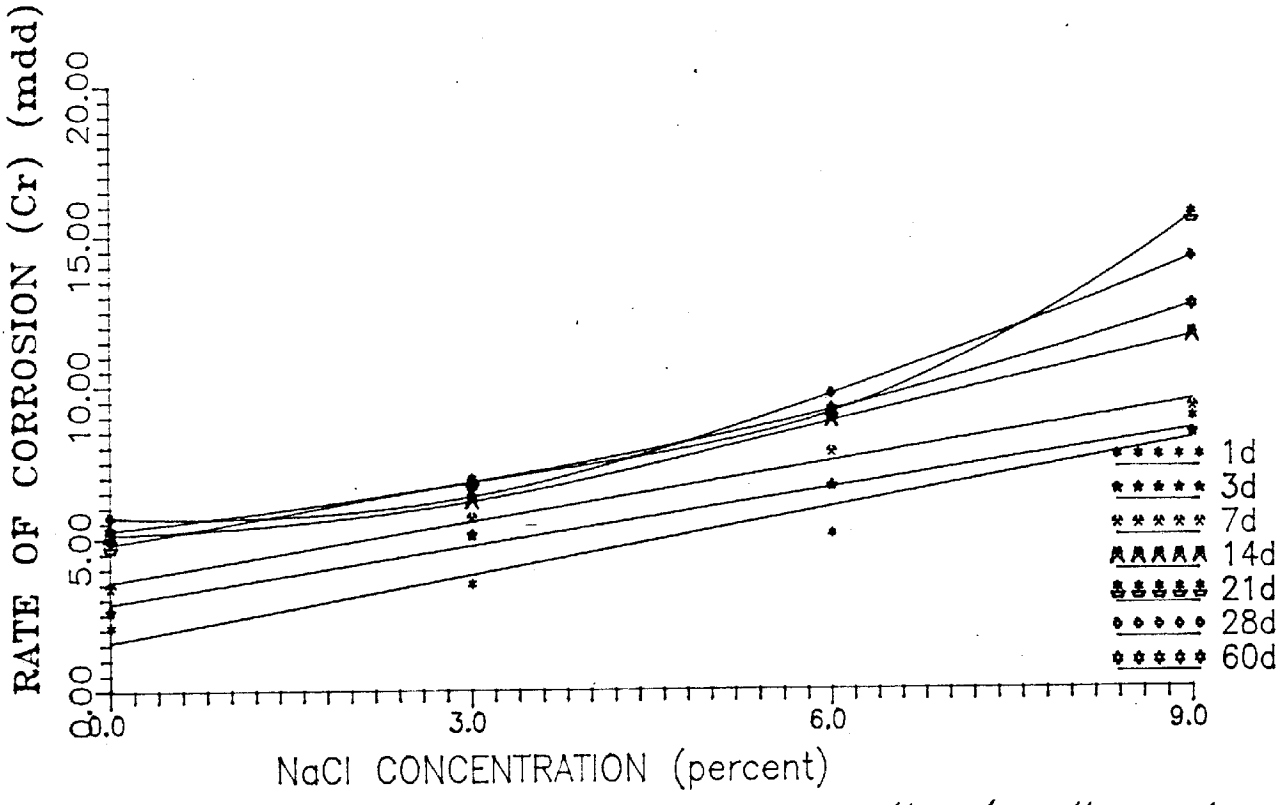

Fig 4.25 Cr Vs % salt solution curves 1:3 mix (alternate wetting & drying con-itio

CHAPTER - V

CONCLUSIONS AND SCOPE FOR FURTHER WORK

5.1 GENERAL

The conclusions drawn from the limited experimental work undertaken and the scope for further research are summarised below. Because of the short time period available, accelerated corrosion has been resorted to for inducing higher degrees of corrosion by using salt solutions of 3%, 6% and 9% concentrations for curing of specimens, along with plain water curing for the comparison of the results obtained.

5.2 CONCLUSIONS

Based on the experimental work undertaken, the following conclusions are drawn :

(i) The cracking strength stabilises after an initial peak over a short period at values 75-90% of the peak strengths. Therefore, for adopting a safe value, the design strength of ferrocement may be taken as 70% of the peak values at 28 days, which corresponds to a material partial safety factor of 1.5 . Thus, for design purposes, the first cracking stress in bending (σ_{crb}) can be estimated by the following expression :

$$\sigma_{crb} = \frac{1}{1.5} (28.02\ S_{LT} + \sigma_{mr}) \qquad \text{in MPa}$$

where S_{LT} is the specific surface of the reinforcement in mm^{-1} and σ_{mr} is the modulus of rupture of the mortar in MPa .

(ii) The effect of cumulative corrosion does not result in any appreciable loss of cracking strength unless C_e assumes a very high value, i.e. C_e = 700md, at which the decrease is 15-25% of the peak strength .

(iii)Excessive corrosion results in lowering of the yield strength of the meshes, lowers the load factor and affects the trilinear load-deflection behaviour of the composite. In this study, the load factors were generally lying in the range of 1.59 to 1.97 . Therefore, a pertial safety factor of 1.5 can be adopted on the loads for design based on the deflection criteria only.

(iv) Excessive corrosion causes the reduction of the cracked range in the stress-strain curve of the composite. It also causes reduction in the ultimate strain value and thereby in the ductility or energy absorption capabillity of the composite.

(v) The spontaneous potential test results suppoert the result obtained from the strength and corrosion tests and clearly show the progress of the corrosion in the samples. The corrosion of the galvanizing layer drops the potential value to around -0.1 V. The effect of the galvanizing layer is to shift the threshold limit of corrosion upwards by about 0.3 V. The corrosion of steel sharply drops the potential values in the final stages.

(vi) Alternate wetting and drying causes 10-20 % higher corrosion than that under submerged condition, which is more prominent in the case of plain water curing. The rate of corrosion generally increases with time.

(vii)The studies indicate the necessity of using rich mortar-1:1.5 to 1:2 mix with a water cement ratio preferably less than 0.45. More side covers should be provided and surface or form vibrators should be used for compaction, wherever possible.

(viii)The galvanizing layer of the commercially available wire mesh is protective enough only in the case of plain water curing. For corrosive ion environments, a double galvanizing layer may be

provided. Use of stainless steel meshes as an option would be very costly. A cheaper alternative could be the use of 100-300 ppm CrO_3 (Chromium trioxide) may be added in the mixing water while preparing the mortars , as proposed by the Christensen (11).

5.3 SCOPE FOR FURTHER WORK

For any continuing research work, the following suggestions are made :

(i) Corrosion studies should be carried out over a longer time period.

(ii) The non-destructive corrosion test, i.e. spontaneous potential test could be used for assessing the extent of corrosion on existing structures, using copper-copper sulphate and other electrodes.

(iii) More data is required on the corrosion of a galvanized wire mesh and its effect on the Pourbiax diagram of iron.

(iv) The effect of different aggressive environments like sulphates and other chlorides on the behaviour of ferrocement could be studied.

REFERENCES

1. Collen, L.D.G. and Kirwan, R.W., "Some Notes on the Characteristics of Ferrocement", Civil Engineering and Public Works Review, Feb. 1959, Vol.54, pp. 195-196 .

2. Rao,A.K. and Gowder,C.S.K., "A Study of the Behaviour of Ferrocement in Flexure", The Indian Concrete Journal, Vol.45, No.4, April 1971, pp.178-183.

3. Desayi,P. and Jacob,K.A.,"Strength and Behaviour of Ferrocement in Tension and Flexure", Proceedings of the Symposium on Modern Trends in Civil Engineering, University of Roorkee,Roorkee, Nov.1972, pp.274-279 .

4. Logan,D. and Shah,S.P.,"Moment Capacity and Cracking Behaviour in Flexure ",ACI Journal ,Proceedings, Vol.70, No.12, Dec.1973, pp.799-804 .

5. Johnston,C.D. and Mowat,D.N.,"Ferrocement-Material Behaviour in Flexure ",Journal of the Structural Division, Proceedings ASCE, Vol.100, No.ST10, Oct.1974, pp.2071-2090 .

6. Surya Kumar,G.V. and Sharma,P.C.,"An Investigation of the Ultimate and First Crack Strength of Ferrocement in Flexure", Indian Concrete Journal, Nov.1976,pp.335-340 & 344 .

7. Balaguru,P.N. ,Naaman,A.E. and Shah,S.P.,"Analysis and Behaviour of Ferrocement in Flexure", Journal of Structural Engineering Division, Proceedings ASCE, Vol.103, No.ST10, October 1977, pp.1937-1951 .

8. Yen,T. and Su,C.F., "Influence of Skeletal Steel on the Flexural Behaviour of Ferrocement", Journal of Ferrocement, Vol.10, No.3, July 1980, pp.177-188 .

9. Mansur,M.A. and Paramasivam,P.,"Cracking Behaviour and Ultimate

Strength of Ferrocement in Flexure",Proceedings of the Second International Symposium on Ferrocement, Bangkok, 1985, pp.47-59 .

10. Kaushik,S.K. ,Trikha,D.N. and Kotdawala,R.R.,"Ultimate Strength Behaviour of Ferrocement Beams", RILEM/ISMES International Symposium on Ferrocement, Bergamo, Italy, 1981, pp.2/115-2/126 .
11. Christensen,K.A. and Williamson,R.B. ,"Solving the Galvanic Cell Problem in Ferrocement", Report No.UC SE SM 71-14, University of California, Berkeley, U.S.A, 1971 .
12. Greenuis,A.W., "Ferrocement for Canadian Fishing Vessel", No.88, Technical Report Series of the Industrial Development Branch, Fisheries and Marine Service, Environment, Canada, 1975 .
13. Naaman,A.E. and Sabins,G.M. ,"Tentative Guidelines for the Use of Ferrocement in Some Structural Applications",Proceedings of the International Conference on Materials of Construction for Developing Countries, Bangkok, Thailand, pp.677-688 .
14. Bigg,G.W. ,"An Introduction to Design for Ferrocement Vessels", Industrial Development Branch, Fisheries Service, Canada, 1972 .
15. Mathews,M.S. ,Achyutha,H. and Rao,P.S. ,"Environment Effects on Cracked Ferrocement ",Proceedings of the Asia-Pacific Symposium on Ferrocement Applications for Rural Development, Roorkee, India, 1984, pp.217-220 .
16. Trikha,D.N., Sharma,S.P. ,Kaushik,S.K. ,Sharma,P.C. and Tewari,V.K. ,"Corrosion Studies of Ferrocement Structures", Journal of Ferrocement, Vol.14, No.3, July 1984, pp.221-233 .
17. Selvi Rajkumari,S. ,Neelamegam,M. ,Rajmane,N.P. and Peter,J.A.,"Effect of Sea Water on Ferrocement With and Without Polymer Impregnation", Proceedings of the Second International

Symposium on Ferrocement, Bangkok, January 1985, pp.681-688 .

18. Chowdhury,S.M.M.I. and Nimityongskul ,"Some Aspects on Corrosion of Galvanized Wire Mesh in Ferrocement Under Simulated Adverse Environments ",Proceedings of the Second International Symposium on Ferrocement, Bangkok, January 1985, pp.689-700 .

19. Ravindrarajah,S.R. and Paramasivam,P. ,"Influence of Weathering on Ferrocement Properties", Proceedings of the Second International Symposium on Ferrocement, Bangkok, January 1985, pp.75-88 .

20. Yozuqullu,O. ,"Durability of Sulfur Impregnated Precast Ferrocement Elements", Journal of Ferrocement, Vol.16, No.4, October 1986 ,pp.429-435 .

21. Irons,M.E. ,"Corrosion and Corrosion Prevention in Ferrocement Hulls", Journal of Ferrocement, Vol.14, No.2, April 1984, pp.159-162 .

22. Sharma,P.C. ,"Coating of Ferrocement Surface", Proceedings of the Second International Symposium on Ferrocement, Bangkok, January 1985 ,pp.641-654 .

23. Tashiro,C. and Ueoka,K. ,"Spontaneous Potential and Microstructure on Corrosion of Steel in Cement Mortar", Proceedings of the Second International Symposium on Ferrocement, Bangkok, January 1985, pp.633-640 .

24. S.Carlos Group, "Steel Corrosion on Ferrocement : Some Notes about Older Construction in S.Carlos, Brazil", Proceedings of the Second International Symposium on Ferrocement, Bangkok, January 1985, pp.607-619 .

25. Paul,B.K. and Pama,R.P. ,"Ferrocement", International Ferrocement Information Centre, Asian Institute of Technology, Bangkok,

Thailand, August 1978 . (Thai Watana Panich Press Co. Ltd.)

26. Trikha, D.N. , Kaushik, S.K., Gupta, V.K., Tewari, V.K. and Sharma, P.C., "Studies on Corrosion Behaviour of Ferrocement Structures", Proceedings of the Second International Symposium on Ferrocement, Bangkok, January 1985, pp.621-632 .

APPENDIX

I. Calulation of First Crack Stress

Load = P kg = P x 9.81 N

Span = 320 mm

Moment, M = (P x 9.81 x 320) / 4 = P x 784.8 N-mm

Section of the sample = 200 mm x 20 mm

Moment of inertia of the section (gross), I = 133333 mm^4

(Using tranformed moment of inertia yeilds only 10% lower stresses)

Cracking stress, $\sigma_{crb} = \frac{M \times t}{I \times 2}$ in MPa

For example : If P = 150 kg, then σ_{crb} = (150 x 784.8 x 20)/(133333 x 2)

= 8.79 MPa

II. Conversion of Electrical Half-cell Potential

Electrical Potential of Standard Hydrogen electrode, V_{she} = 0 V

Electrical Potential of Saturated Calomel electrode, V_{sec} = +0.2415 V

Electrical Potential of Copper-Copper sulphate electrode,

(CSE scale), V_{cse} = -0.316 V

Therefore, to convert a potential value from calomel scale to the CSE scale, subtract 0.5575 V from the value.

Plates

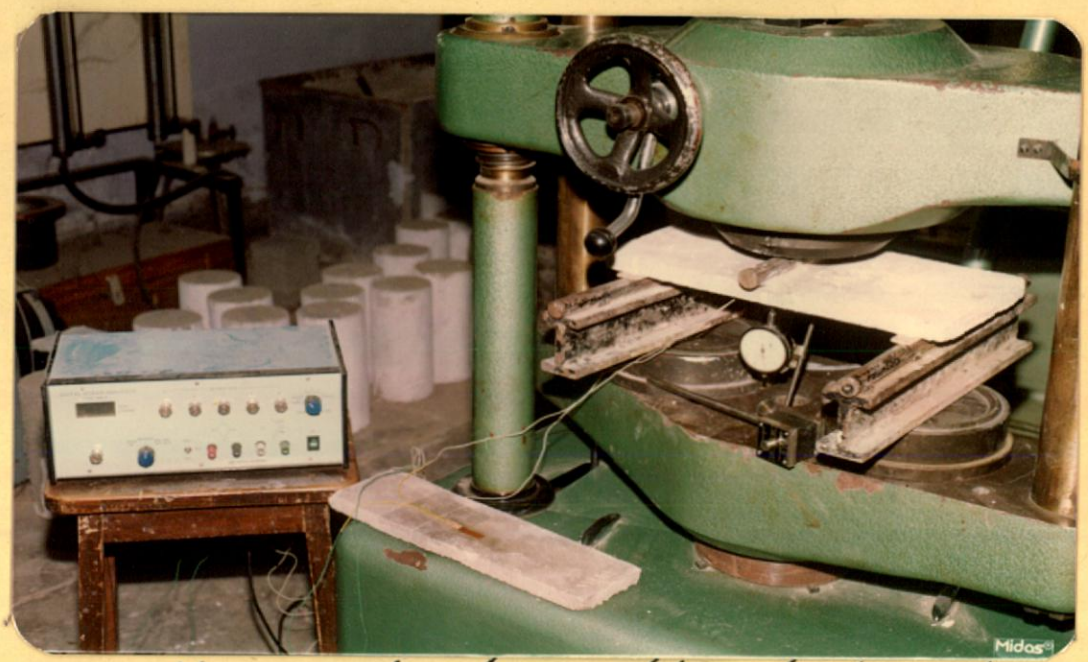

3.1: flexural strength test set-up

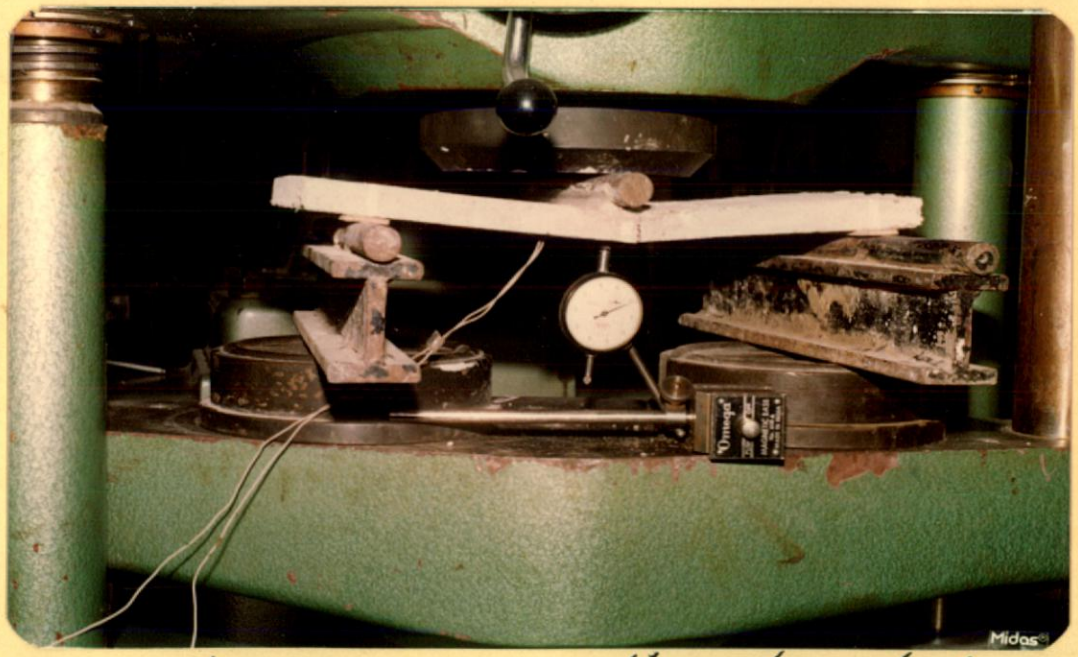

3.2: specimen in ultimate state

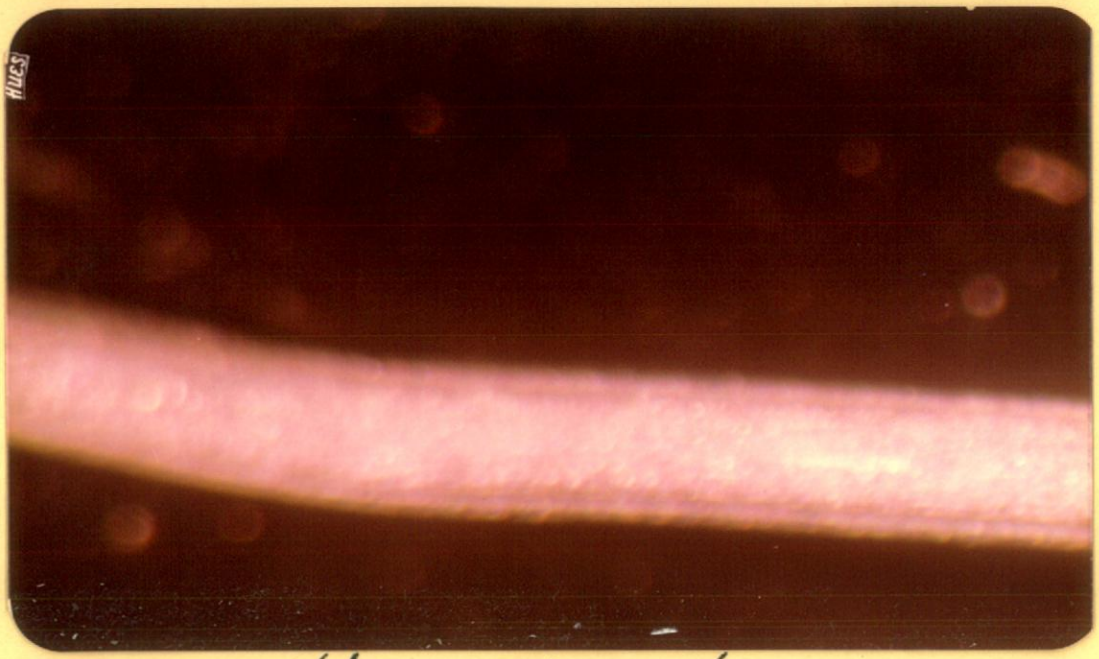

3.3: sample - original

3.4: sample 3/0/14/SB ; C_e = 63.5 md

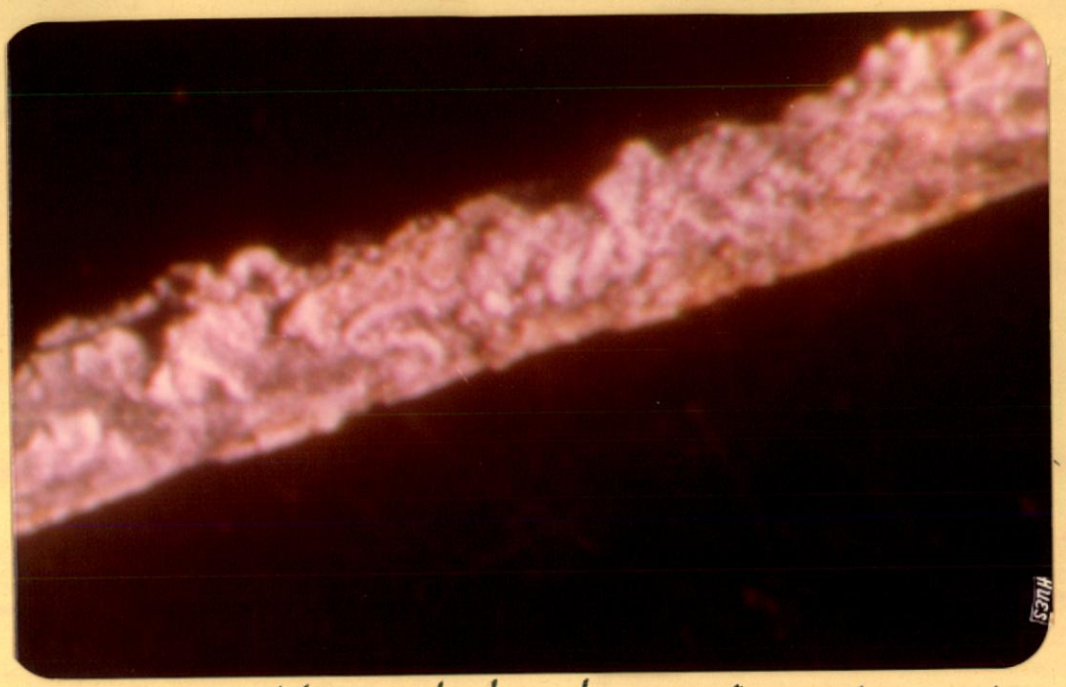

3·5 : sample 3/0/28/SB ; C_e = 142·7 md

3·6 : sample 3/9/14/AW ; C_e = 162·2 md

3·7 : sample 3/6/28/SB; k_e = 181·4 md

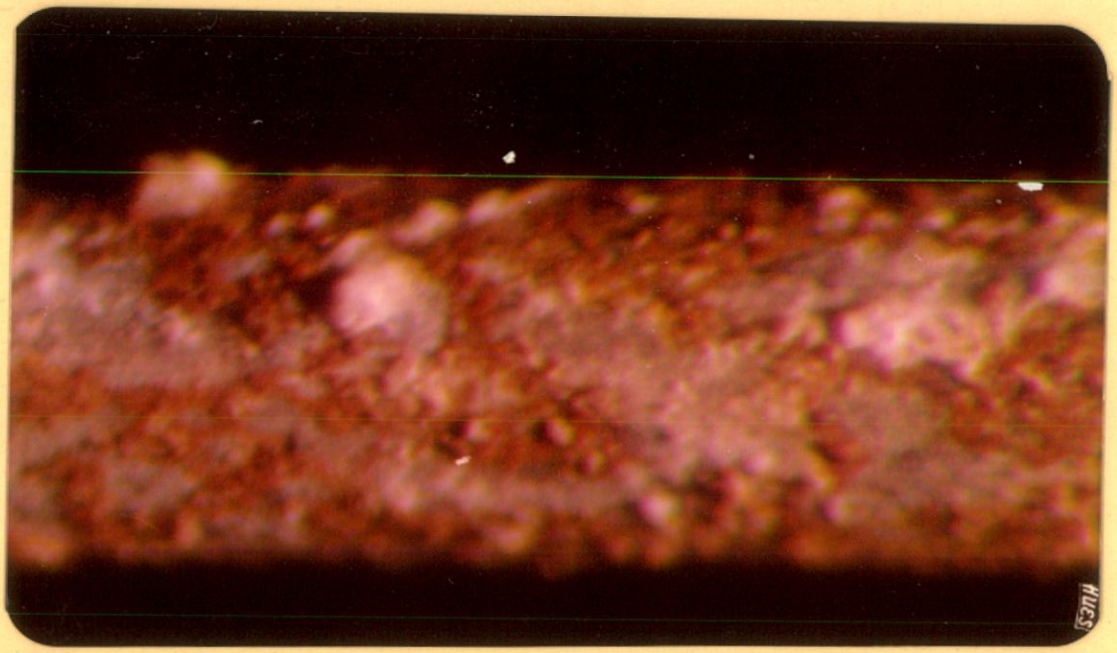

3·8 : sample 1·5/6/28/AW; k_e = 229·4 md

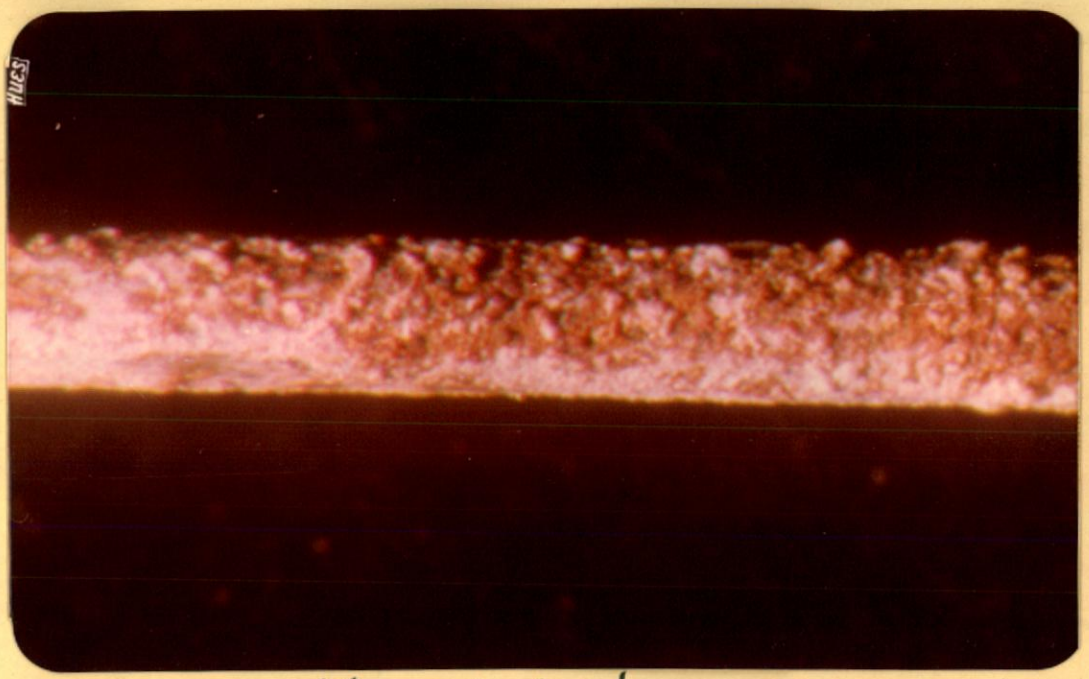

3.9: sample 3/9/21/SB; Ce = 235.6 md

3.10: sample 1.5/0/60/SB; Ce = 248.7 md

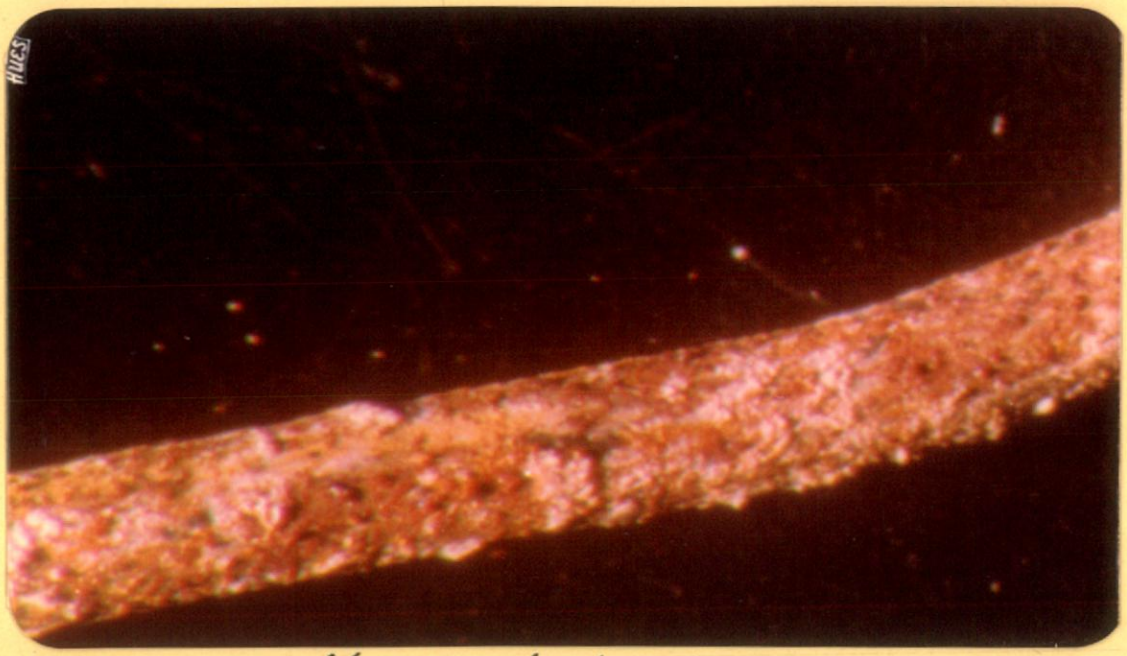

3.11: sample 1.5/9/28/SB ; Ce = 284.6 md

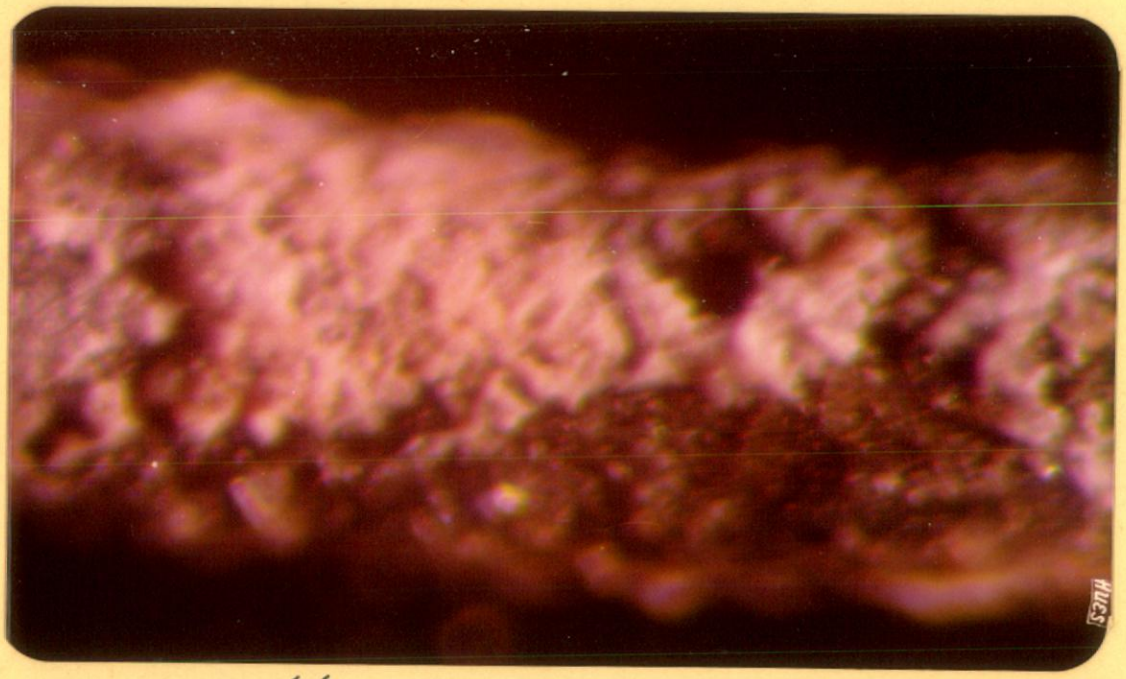

3.12: sample 3/0/60/SB ; Ce = 296.9 md

3·13 : sample 1·5/3/60/SB ; Ce = 348·3 md

3·14 : sample 3/6/60/SB ; Ce = 558·5 md